

The electronic absorption spectra of mono- and bis-azo dyes in ethanol :

The electronic absorption spectra of hydroxy or carboxyphenylazoacetylacetone derivatives or benzene-bis-azoacetylacetone derivatives in ethanol are shown in Figs. (1-4). The spectral data are given in Table (2). The spectra of compounds under investigation comprise mainly two or three absorption bands within the region 200-500 nm. The spectra of I_{a-c} exhibit three bands, the first band at 216, 216 and 217 nm has ϵ_{\max} amounting to 0.88×10^4 , 1.08×10^4 and 1.7×10^4 mol⁻¹. L. cm⁻¹ for I_a , I_b , I_c respectively. This band is attributed to the transition (${}^1L_a \leftarrow {}^1A$) state of the phenyl ring. The second band at 250, 245 and 240 nm has ϵ_{\max} amounting to 1.06×10^4 , 1.1×10^4 and 1.78×10^4 mol⁻¹. L. cm⁻¹ for I_a , I_b , I_c respectively. This second band has high extinction value and is solvent insensitive, thus it is attributed to the transition (${}^1L_b \leftarrow {}^1A$) of the phenyl ring. The compounds I_a , I_b , I_c show at longer wavelength a third band at 403, 414 and 431 nm with ϵ_{\max} amounting to 2.41×10^4 , 2.17×10^4 and 2.22×10^4 mol⁻¹. L. cm⁻¹ respectively. This band is very sensitive to solvent polarity and varies from I_a to I_c , Table 2, by varying the substituent from methyl to phenyl groups in the pentanedione part of the molecule. From the latters, the third band is probably of the charge transfer type. The spectral data for third band reveal a red shift and variation in extinction from I_a to I_c when methyl group replaced by phenyl ring in the compound.

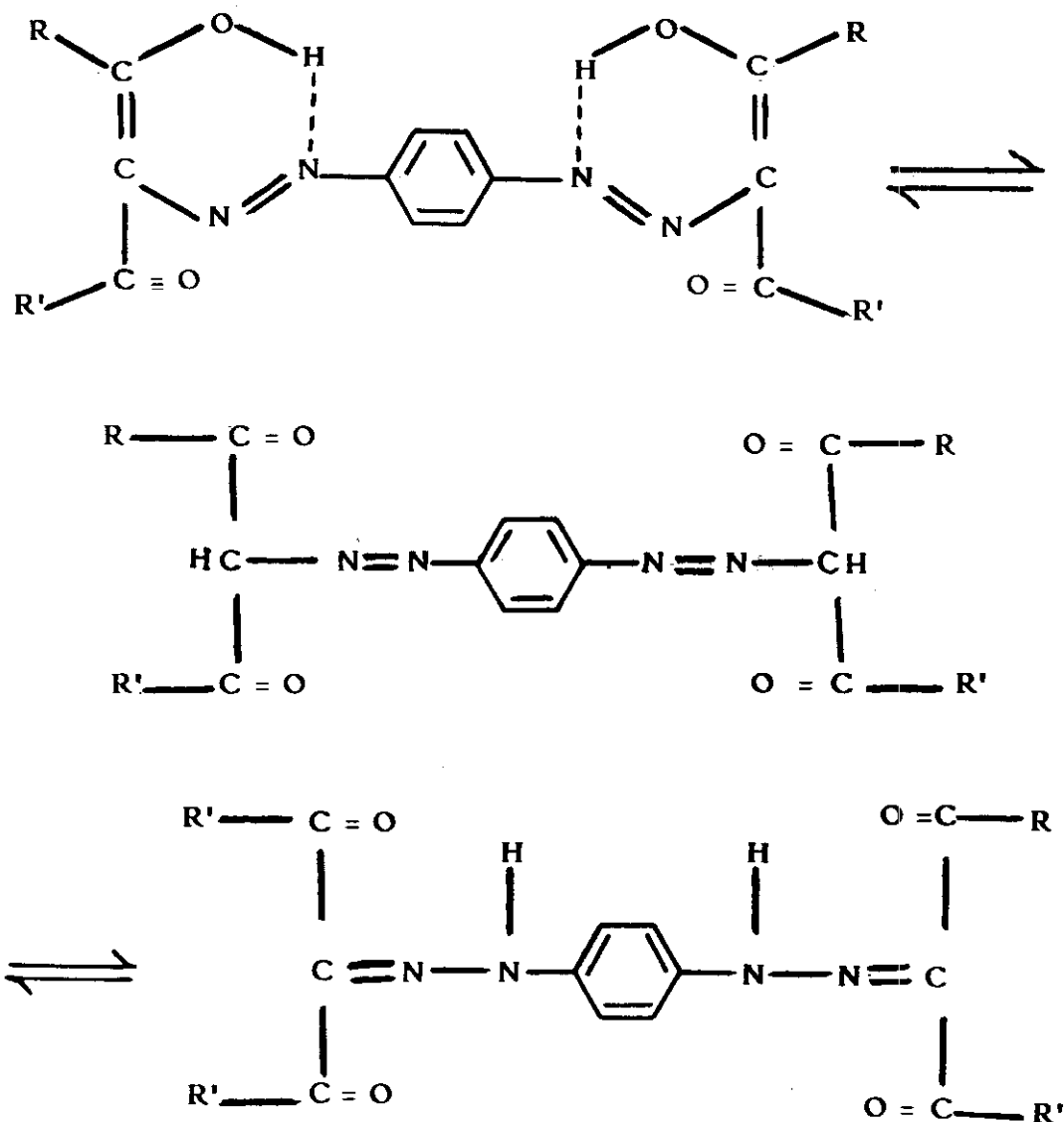
Spectra of compounds II_a , II_b and II_c show one band at 229 nm which is due to (${}^1L_a \leftarrow {}^1A$) transition of phenyl ring; also these compounds exhibit a second band at 252, 255 and 258 nm with ϵ_{\max} amounting to 1.22×10^4 , 1.27×10^4 and 1.93×10^4 mol⁻¹. L. cm⁻¹ respectively. This second

band which is more or less insensitive to solvent polarity, may due to transition (${}^1L_b \leftarrow {}^1A$) of the phenyl ring. The compounds II_a, b, c exhibit also a longer wavelength band at 364, 376 and 388 nm with ϵ_{\max} amounting to 2.2×10^4 , 1.88×10^4 and 2.12×10^4 $\text{mol}^{-1} \cdot \text{L} \cdot \text{cm}^{-1}$ respectively. This band shows a red shift on going from II_a to II_c i.e on substituting the methyl group by a phenyl one in the pentanedione part of the molecule. At the same time the band is highly sensitive to the solvent polarity which confirms its CT nature.

The spectra of the ethanolic saturated solution of compounds III_a, b, c give three bands. The first one, located at 212, 213 and 212 nm, can be assigned to (${}^1L_a \leftarrow {}^1A$) state of the phenyl ring. The second band at 244, 247 and 249 nm for III_a, b, c respectively is practically insensitive to solvent polarity and may be attributed to the transition (${}^1L_b \leftarrow {}^1A$) of the phenyl ring. The third band at longer wavelength for III_a, III_b and III_c are a broad band shown at 374, 383 and 404 nm respectively. The position of this band is very sensitive to the solvent polarity and also to the type of the substituent on the pentanedione part of the molecule. Another broad band of III_a at longer wavelength but of low extinction (located at ≈ 480 nm) may be attributed to a charge transfer of another type within the molecule.

The spectra of ethanolic saturated solution of the compounds IV_a and IV_b exhibit three bands, the first one at 216 and 215 nm is attributed to the transition (${}^1L_a \leftarrow {}^1A$). The second band located at 252 and 245 nm is insensitive to the nature of solvents and attributed to (${}^1L_b \leftarrow {}^1A$) transition

of the phenyl ring. The third band at 430 and 440 nm for IV_{a, b} shows a variation in λ_{\max} with change of the CH₃ group of the pentanedione part of the molecule by phenyl ring and is very sensitive to the solvent polarity. This band can be assigned to a charge transfer interaction within the molecule. From Fig. (4) it can be seen that the CT band of compound IV_a is a composite one whereas it splits to two bands in case of IV_b one of them at 303 nm and the other at 440 nm. This can be attributed to the tautomeric equilibrium of these compounds which can be represented as follows:



generally it is clear from the spectral data Table (2) and Figs (1-4) that λ_{\max} of the CT band of these compounds in ethanol solvent is shifted to longer wavelength on substituting the methyl group by the phenyl ring in the pentane-dione part of the molecule. This is due to the increase of the conjugation and the delocalization of electrons within the molecule.

The electronic absorption spectra of mono- and bis-azo compounds in different organic solvents :

The electronic absorption spectra of mono-azo dyes (I_{a-c} , II_{a-c}) and bis-azo dyes (III_{a-c} , $IV_{a,b}$) are scanned in ethanol, methanol, acetonitrile, acetone, chloroform, ether, dioxane, carbontetrachloride or cyclohexane as given in Figs. (1-4) and the spectral data are shown in Tables (3-6).

The mono- and bis-azo-compounds show a broad band with wide variation in its position with changing the solvent polarity supporting the CT nature of the band overlapped with the $\pi - \pi^*$ transition of the azo group. This CT band is red shifted on going from nonpolar (cyclohexane) to polar (ethanol) solvents but the position of the CT band of the molecule in the visible region of the spectra has no regular variation with changing the nature of the solvent. This is due to the interference of different types of transitions appearing in this region Figs. (1-4). The shift in λ_{\max} can be discussed in terms of the solvent polarity viz dielectric constant and the possibility of formation of an intermolecular hydrogen bond between compound and solvent molecules. Kundt⁽⁶⁶⁾ considered that the solvent refractive index was the determining factor where either the solvent or solute is nonpolar or of low polarity which is the case of cyclohexane

and carbontetrachloride. Taft and Kamlet⁽⁶⁷⁻⁶⁹⁾ consider the total solvent effect to be composed of three independent contribution viz polarity, acidity and basicity and they introduced a corresponding empirical solvent polarity (π) acidity (α) and basicity (β) scales. Kosower⁽⁷⁰⁻⁷⁴⁾ introduced an empirical parameter for the solvation energy on going from the ground to excited state.

The relation which governs this behaviour was given by Gati and Szalay⁽⁷⁵⁾ in the form of

$$\Delta \nu = (a-b) \left(\frac{n^2-1}{2n^2+1} \right) + b \left(\frac{D-1}{D+1} \right)$$

in which a and b are constants depending on the nature of the solute and having the values 4858 cm^{-1} and 1217 cm^{-1} respectively. n is the refractive index and D is the dielectric constant of the medium. According to this relation the plot of $\Delta \nu$ as a function of the term $\frac{D-1}{D+1}$ would be a linear relation if the dielectric force is predominant as shown in Figs. (5,6). The plots indicate that the CT band suffers a bathochromic shift on increasing dielectric constant and the plots are curved not straight lines indicating that the dielectric constant is not the predominant factor causing the band shift. A more precise relation is a function of dielectric constant by Suppan⁽⁷⁶⁾ of the type

$$F(D) = \frac{2(D-1)}{2D+1} \quad \text{or} \quad \phi(D) = \frac{D-1}{D+2}$$

which relating the shift in band position with dielectric constant of the medium. The plots of λ_{max} of the composite band ($\pi - \pi^*$ transition

of N=N group with CT interaction) in the different solvents used against the function $F(D)$ or $\phi(D)$ are shown in Figs. (7-10). These plots are not linear indicating that the dielectric properties of the medium are not the main factor influencing the excitation energy.

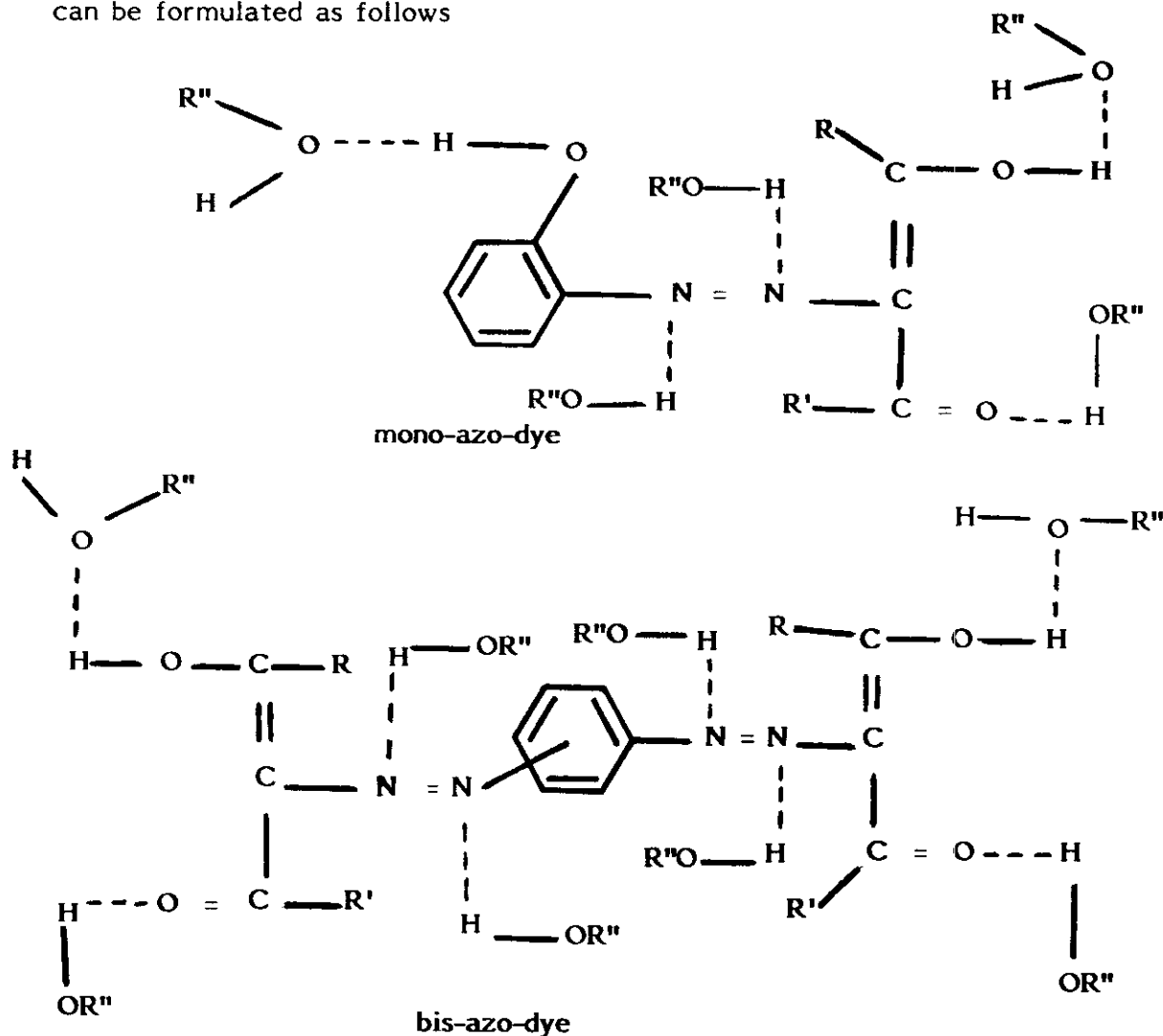
On the other hand, Bayliss⁽⁷⁷⁾ and McRae⁽⁷⁸⁾ derived a multiparameter equation containing the functions $F(n)$ and $F_2(n)$,

$$F(n) = \left(\frac{n^2 - 1}{2n^2 + 1} \right) \quad \text{or} \quad F_2(n) = \left(\frac{n^2 - 1}{n^2 + 2} \right)$$

relating the shift in band position with refractive index of the medium. The plots of $\Delta\nu$ or λ_{\max} of the CT band in different solvents against the two functions $F(n)$ or $F_2(n)$ are shown in Figs. (11,12) and (13,14). These plots are not linear denoting that the refractive index properties of the medium have low effect on the shift of the band.

The plot of λ_{\max} of the CT band for compounds I_{a-c} , II_{a-c} , III_{a-c} and $IV_{a,b}$ in different solvents with other microscopic solvent polarity parameters Z , E_T values and also with the empirical parameters of α or β , which indicate the acidity or basicity of protic and aprotic solvents, are given in Figs. (15-22). The plots give straight lines for relations of λ_{\max} vs. Z and E_T values for all the compounds under investigation except for III_b , III_c which gave a curved line. The linearity of the relation indicates that the solvation properties (or the solute - solvent interaction) consider the main factor affecting the CT band position. The plots of λ_{\max} against α or β values give straight lines for all compounds but deviation from linearity at the curves $\lambda_{\max} - \alpha$ are shown for III_b , IV_a (Fig. 20).

The linearity of the relation indicates that the hydrogen bond donor solvent (α) or hydrogen bond acceptor solvent (β) support the occurrence of the specific association through proton donor-acceptor systems. The formation of hydrogen bond between the solvent and the azo molecules can be formulated as follows



Finally, the shift of the CT band is actually the net resultant effect of the red shift due to increased polarity of the solvent and blue shift due to intermolecular hydrogen bond formed between the solvent molecules and the n -electrons of the azo group or oxygen of the carbonyl group.

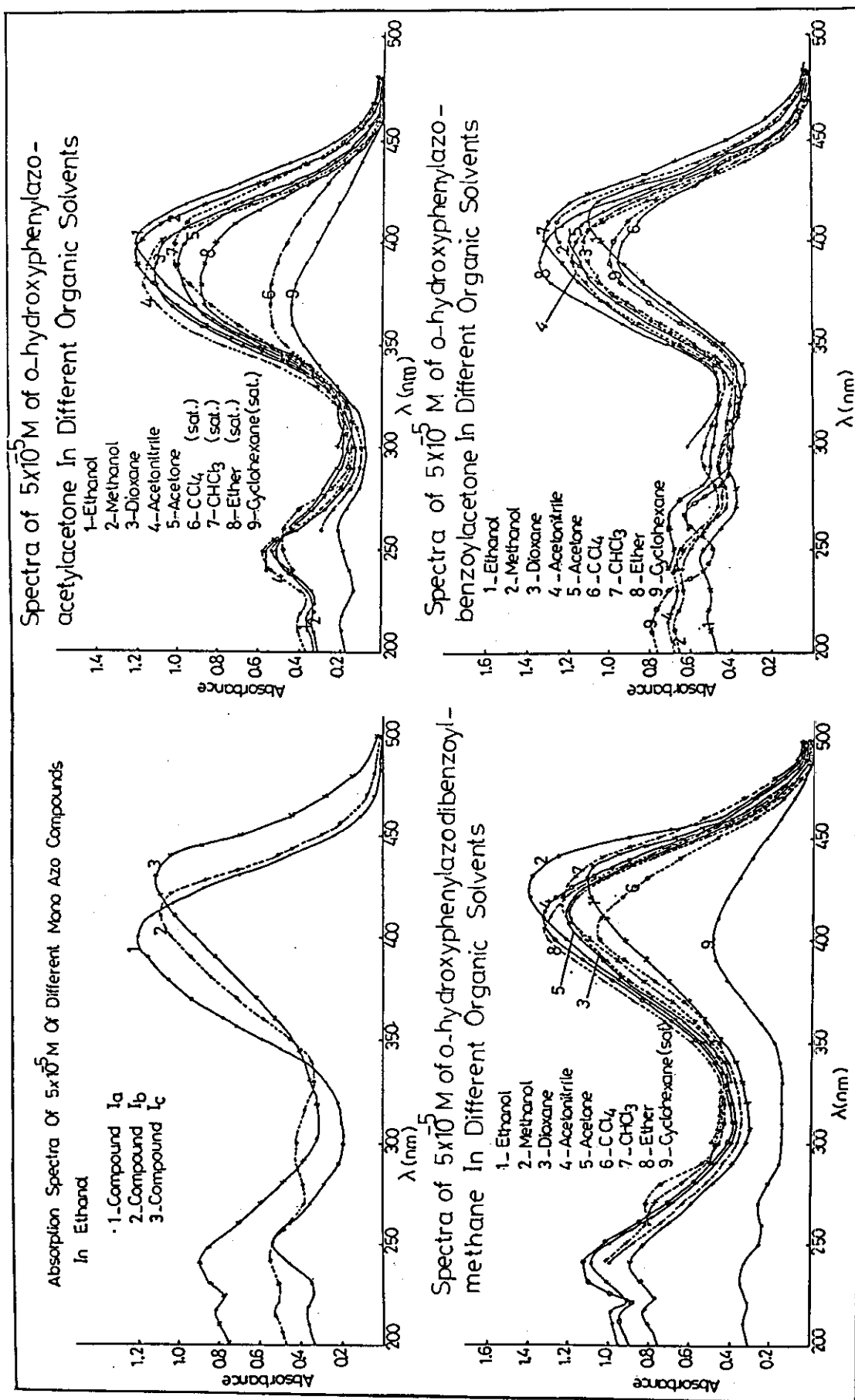


Fig. (1)

Table (3) : Spectral data of compounds I_{a-c} in different organic solvents.

solvent	I _a						I _b						I _c					
	A		B		C		A		B		C		A		B		C	
	λ_{\max} nm	ϵ_{\max} $\times 10^4$	λ_{\max} nm	ϵ_{\max} $\times 10^4$	λ_{\max} nm	ϵ_{\max} $\times 10^4$	λ_{\max} nm	ϵ_{\max} $\times 10^4$	λ_{\max} nm	ϵ_{\max} $\times 10^4$	λ_{\max} nm	ϵ_{\max} $\times 10^4$	λ_{\max} nm	ϵ_{\max} $\times 10^4$	λ_{\max} nm	ϵ_{\max} $\times 10^4$	λ_{\max} nm	ϵ_{\max} $\times 10^4$
acetonitrile	216	0.91	247	1.16	384	2.32	216	1.4	240	1.38	290	0.94	392	2.34	217	2.10	237	2.25
methanol	216	0.89	250	1.07	396	2.39	216	1.36	245	1.35	295	1.08	408	2.49	217	2.0	242	2.17
ethanol	216	0.88	250	1.06	403	2.41	216	1.08	245	1.10	295	0.84	414	2.17	217	1.7	240	1.78
acetone					390	1.98							382 sh 400	2.17 2.36			413	2.42
chloroform			255	—	398	—			265	1.41			402	2.6			270 sh	1.54
ether					380	—							390	2.64			403	2.63
dioxane			245	1.14	388	2.2			250 sh	1.21	290	0.92	399	2.23			413	2.38
CCl ₄					370	—			270	1.24			391	1.88			404	2.11
cyclohexane	216	—	260	—	365	—	216	1.42	230 sh	1.42	267	1.27	389	1.96	217	—	232 270	—

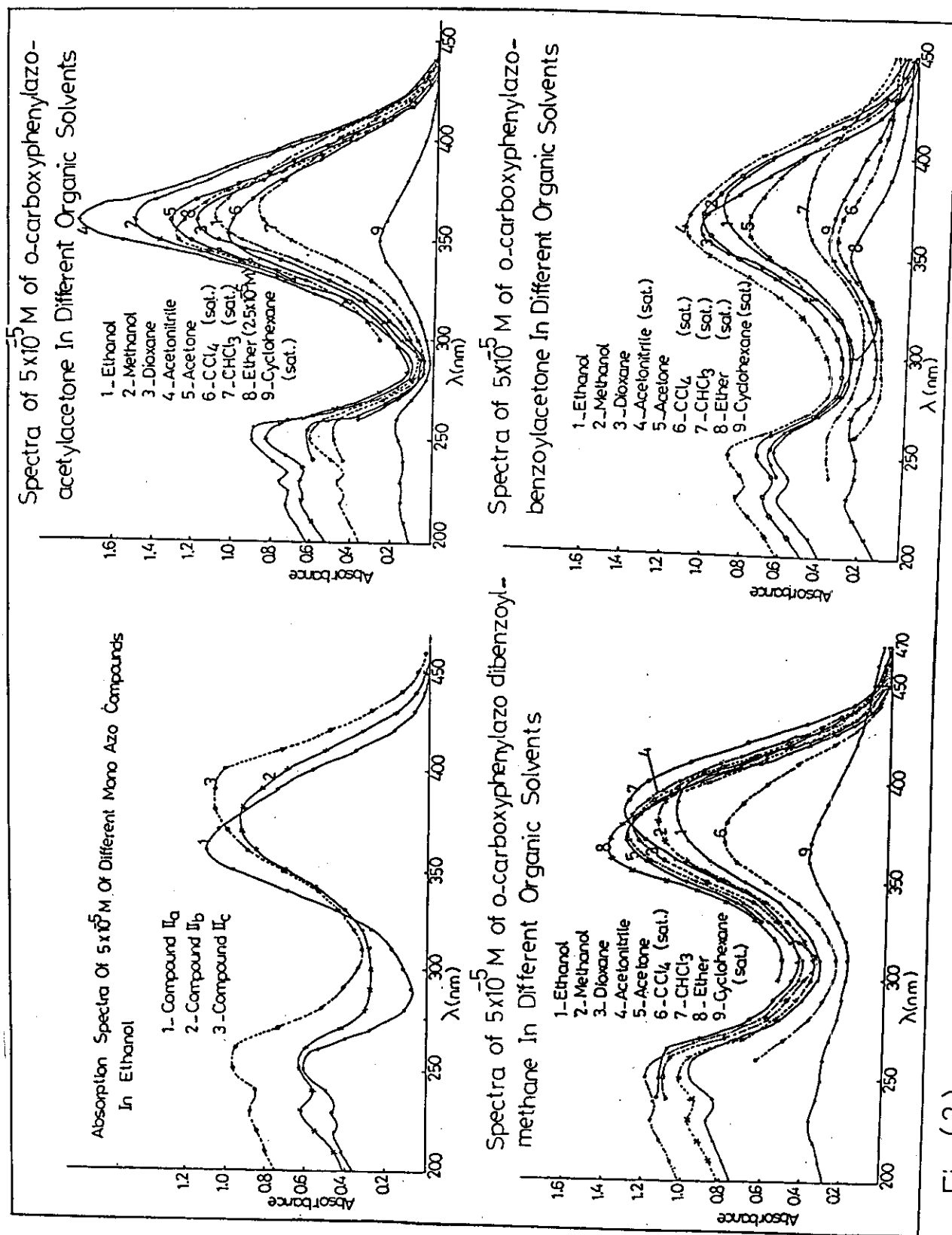


Fig.(2)

Table (4) : Spectral data of compounds II_{a-c} in different organic solvents

solvent	II _a									II _b									II _c								
	A			B			C			A			B			C			A			B			C		
	λ_{\max} nm	ϵ_{\max} $\times 10^4$	λ_{\max} nm	ϵ_{\max} $\times 10^4$	λ_{\max} nm	ϵ_{\max} $\times 10^4$	λ_{\max} nm	ϵ_{\max} $\times 10^4$	λ_{\max} nm	ϵ_{\max} $\times 10^4$	λ_{\max} nm	ϵ_{\max} $\times 10^4$	λ_{\max} nm	ϵ_{\max} $\times 10^4$	λ_{\max} nm	ϵ_{\max} $\times 10^4$	λ_{\max} nm	ϵ_{\max} $\times 10^4$	λ_{\max} nm	ϵ_{\max} $\times 10^4$	λ_{\max} nm	ϵ_{\max} $\times 10^4$	λ_{\max} nm	ϵ_{\max} $\times 10^4$			
acetonitrile	229	1.52	254	1.8	360	3.56	229	—	251	—	—	366	—	229	2.32	251	2.38	375	2.6								
methanol	229	1.32	252	1.66	361	3.0	229	1.38	253	1.46	2.06	370	2.06	229	1.95	253	2.04	383	2.31								
ethanol	229	0.93	252	1.22	364	2.2	229	1.24	255	1.27	1.88	376	1.88	229	1.76	258	1.93	388	2.12								
acetone					359	2.64					1.62	366						373	2.63								
chloroform			255	—	365	—			260	—	—	360	—			260	2.21	385	2.61								
ether					353	5.16					—	352	—					265	2.78								
dioxane			255	1.25	360	2.37			250	1.34	2.10	365	2.10			253	2.2	378	2.54								
CCl ₄					352	—					—	375	—					370	—								
cyclohexane	229	—	259	—	350	—	229	—	268	—	—	354	—	229	—	260	—	360	—								

 $\epsilon_{\max} (\text{mol}^{-1} \text{L.cm}^{-1})$

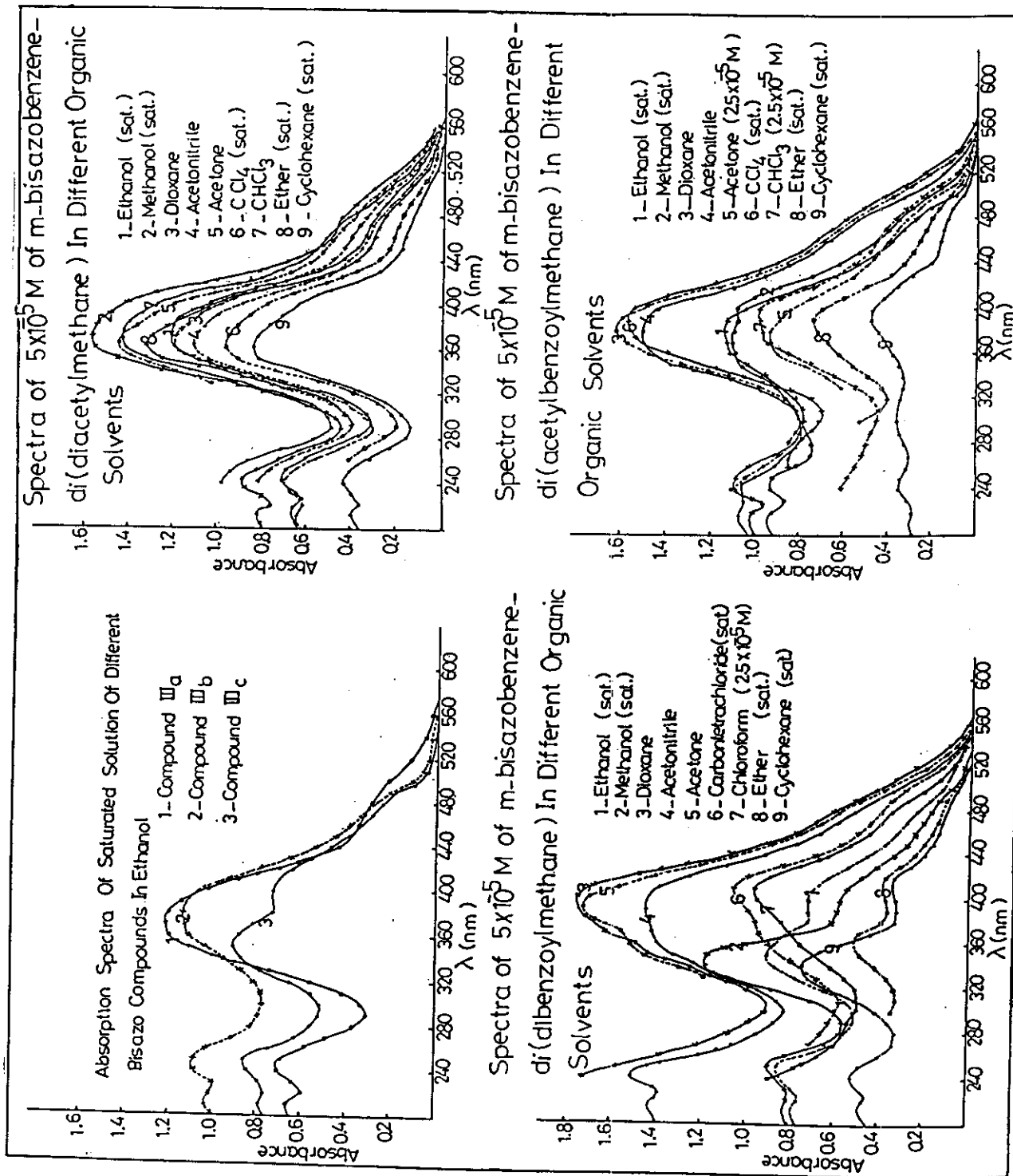
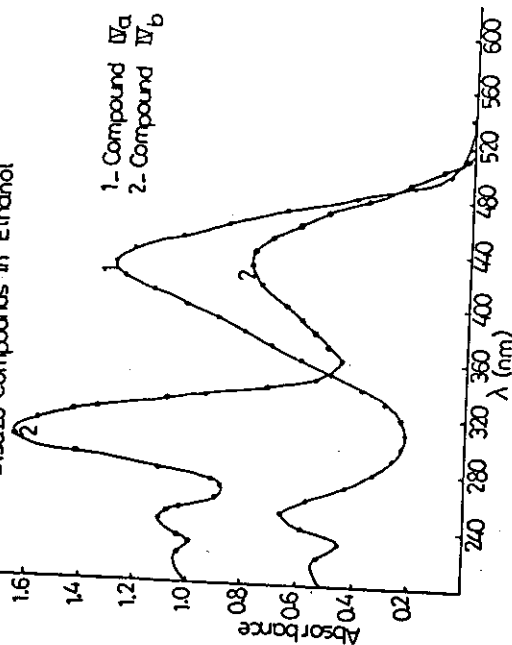
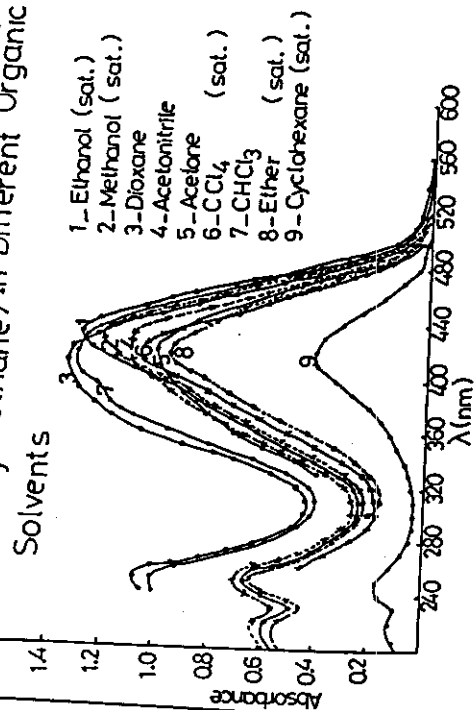


Fig.(3)

Absorption Spectra Of Saturated Solution Of Different Bisazo Compounds In Ethanol



Spectra of 5×10^{-5} M of p-bisazobenzene-di(diacetylmethane) In Different Organic Solvents



Spectra of 5×10^{-5} M of p-bisazobenzene-di(acetylbenzoylmethane) In Different Organic Solvents

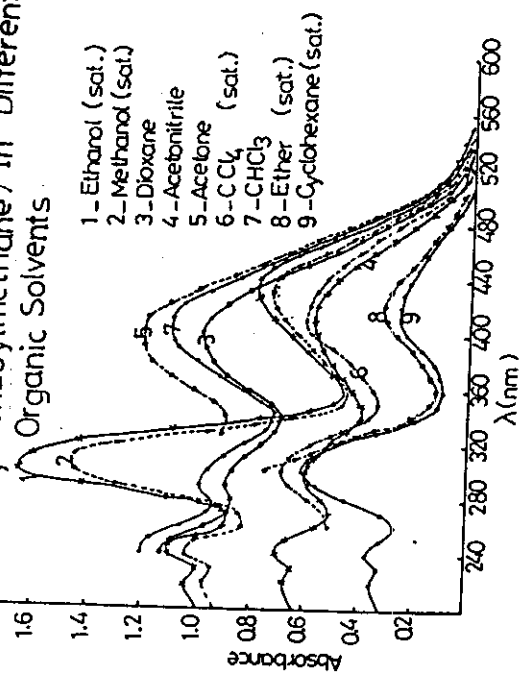


Fig.(4)

Table (6) : Spectral data of compounds IV_{a,b} in different organic solvents

a,b

solvent	IV _a										IV _b							
	A		B		C		D		A		B		C		D			
	λ_{\max} nm	ϵ_{\max} $\times 10^4$	λ_{\max} nm	ϵ_{\max} $\times 10^4$	λ_{\max} nm	ϵ_{\max} $\times 10^4$	λ_{\max} nm	ϵ_{\max} $\times 10^4$	λ_{\max} nm	ϵ_{\max} $\times 10^4$	λ_{\max} nm	ϵ_{\max} $\times 10^4$	λ_{\max} nm	ϵ_{\max} $\times 10^4$	λ_{\max} nm	ϵ_{\max} $\times 10^4$		
acetonitrile	216	1.27	248	1.41	390 _{sh}	1.9	421	2.23	215	1.34	240	1.4	298	1.2	404	1.14		
methanol	216	—	250	—	380 _{sh}	—	428	—	215	—	243	—	305	—	431	—		
ethanol	216	—	252	—	383 _{sh}	—	430	—	215	—	245	—	303	—	440	—		
acetone					379 _{sh}	1.7	418	2.02							401	2.41		
chloroform			250	2.03	382 _{sh}	2.4	409	2.62			250 _{sh}	2.36	292	1.98	406	2.2		
ether							416	—							415	—		
dioxane			252	2.16	390 _{sh}	2.6	411	2.68			250 _{sh}	2.18	290	1.78	400	1.97		
CCl ₄					380 _{sh}	—	415	—					300	—	410	—		
cyclohexane	216	—	245	—	355 _{sh}	—	415	—	215	—	240	—	302	—	410	—		

$$\epsilon_{\max} \text{ (mol}^{-1} \text{ L.cm}^{-1} \text{)}$$

sh = shoulder

The Relation Between $\Delta\bar{\nu}$ And $\frac{D-1}{D+1}$ Values
For C.T. Band of Mono-Azo-Compounds

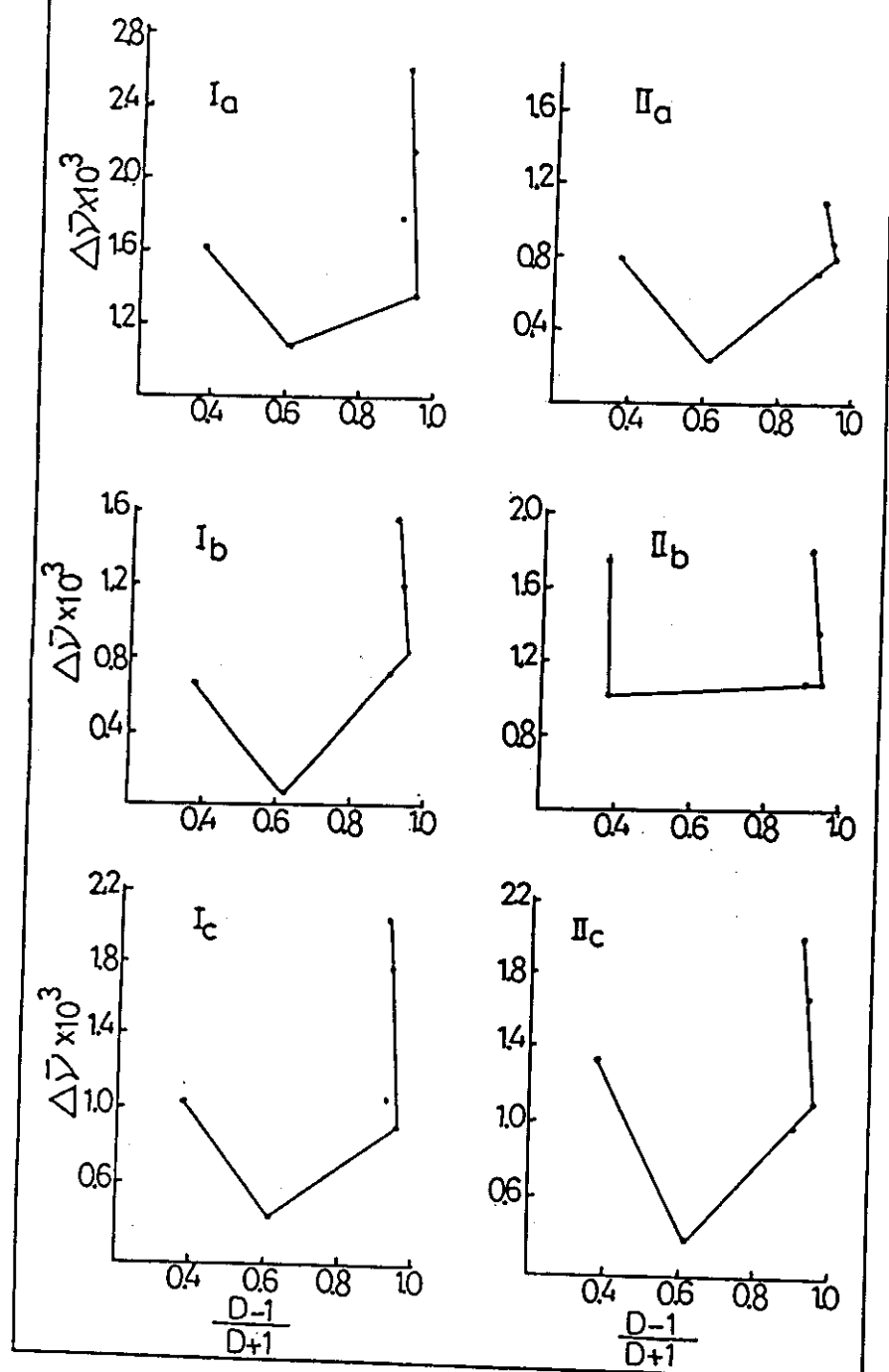


Fig.(5)

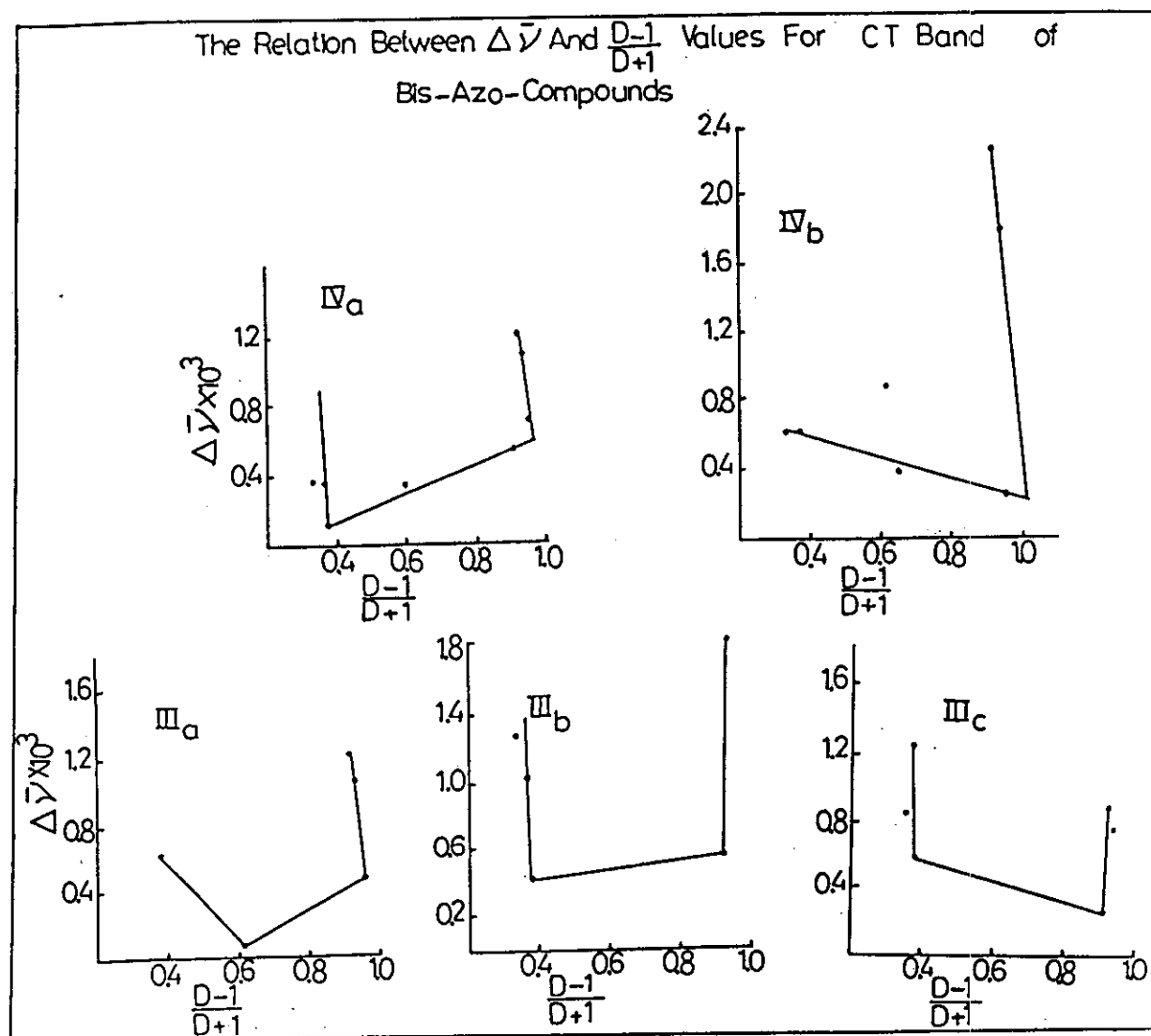


Fig.(6)

The Relation Between λ_{\max} And $f(D)$
Values For CT Band of Mono-Azo -
Compounds

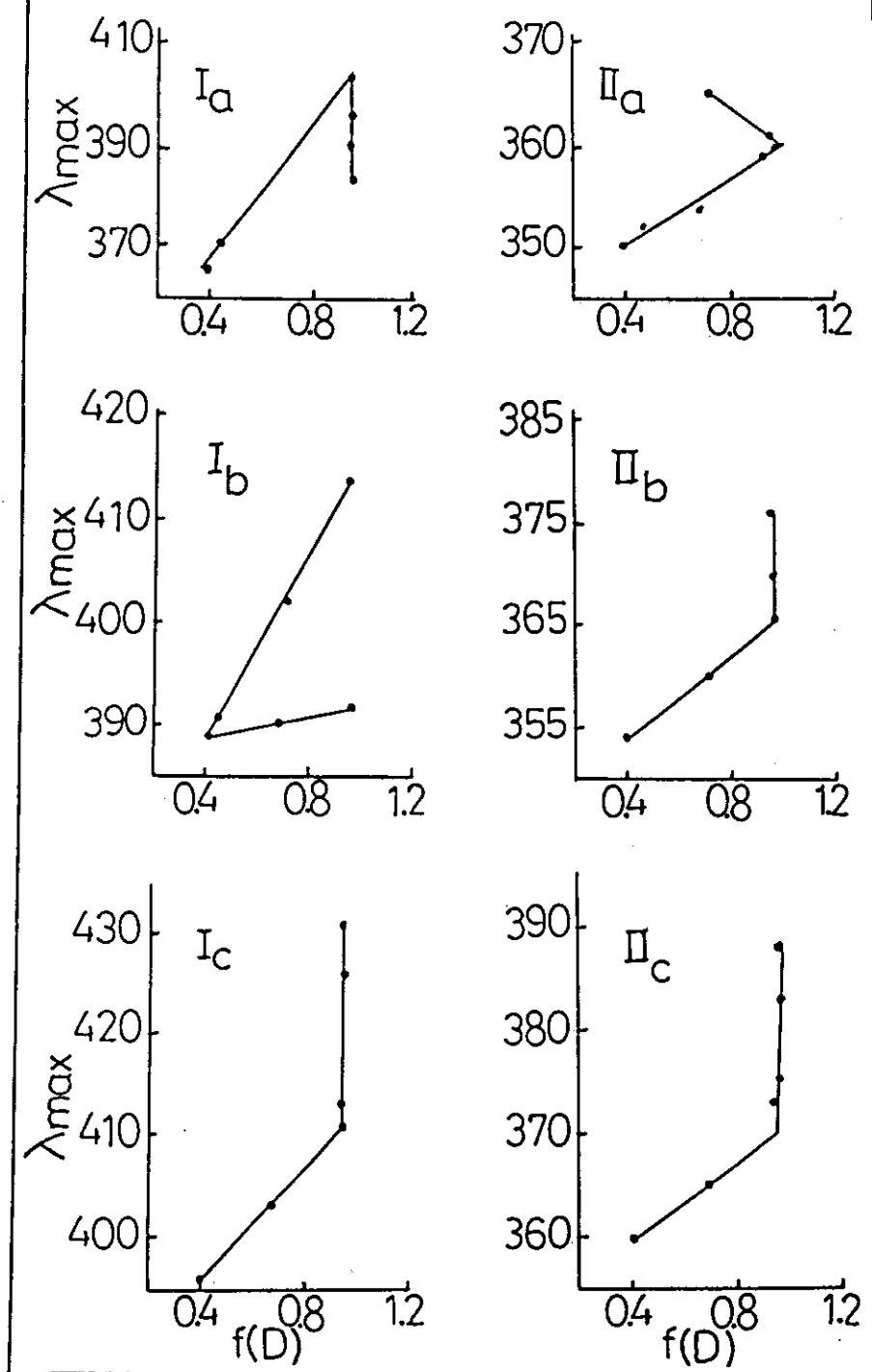


Fig.(7)

The Relation Between λ_{\max} And $f(D)$ Values For
CT Band of Bis-Azo-Compounds

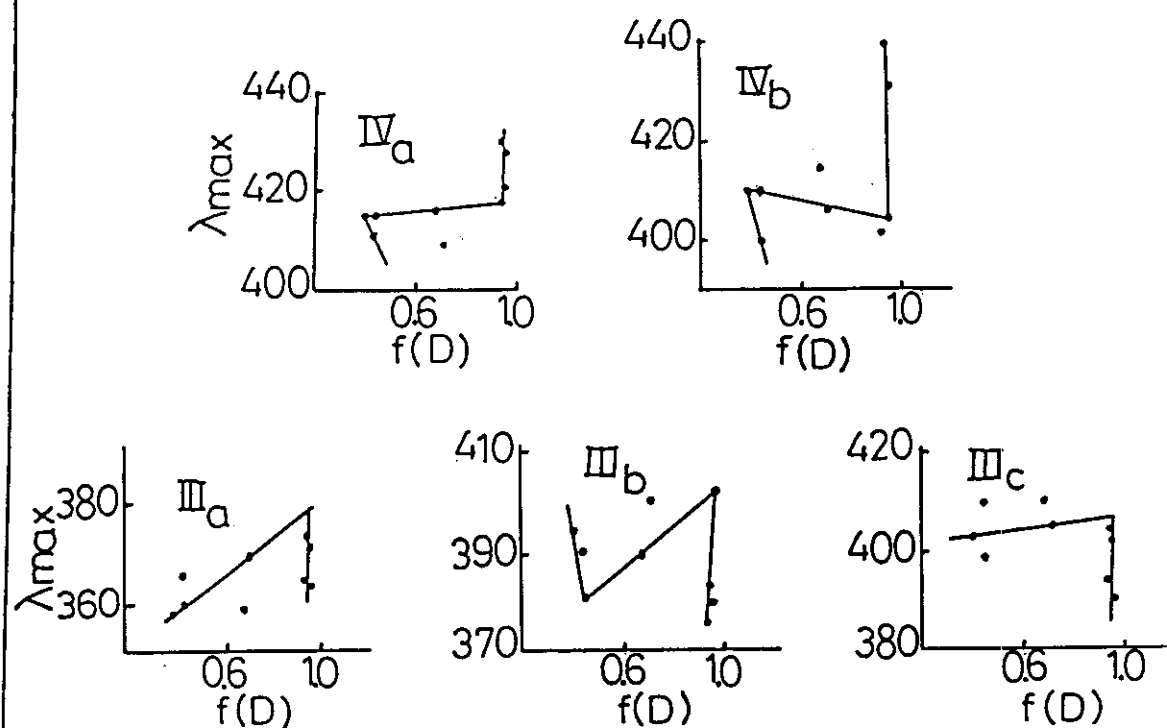


Fig.(8)

The Relation Between λ_{\max} And $\phi(D)$
Values For CT Band of Mono-Azo-
Compounds

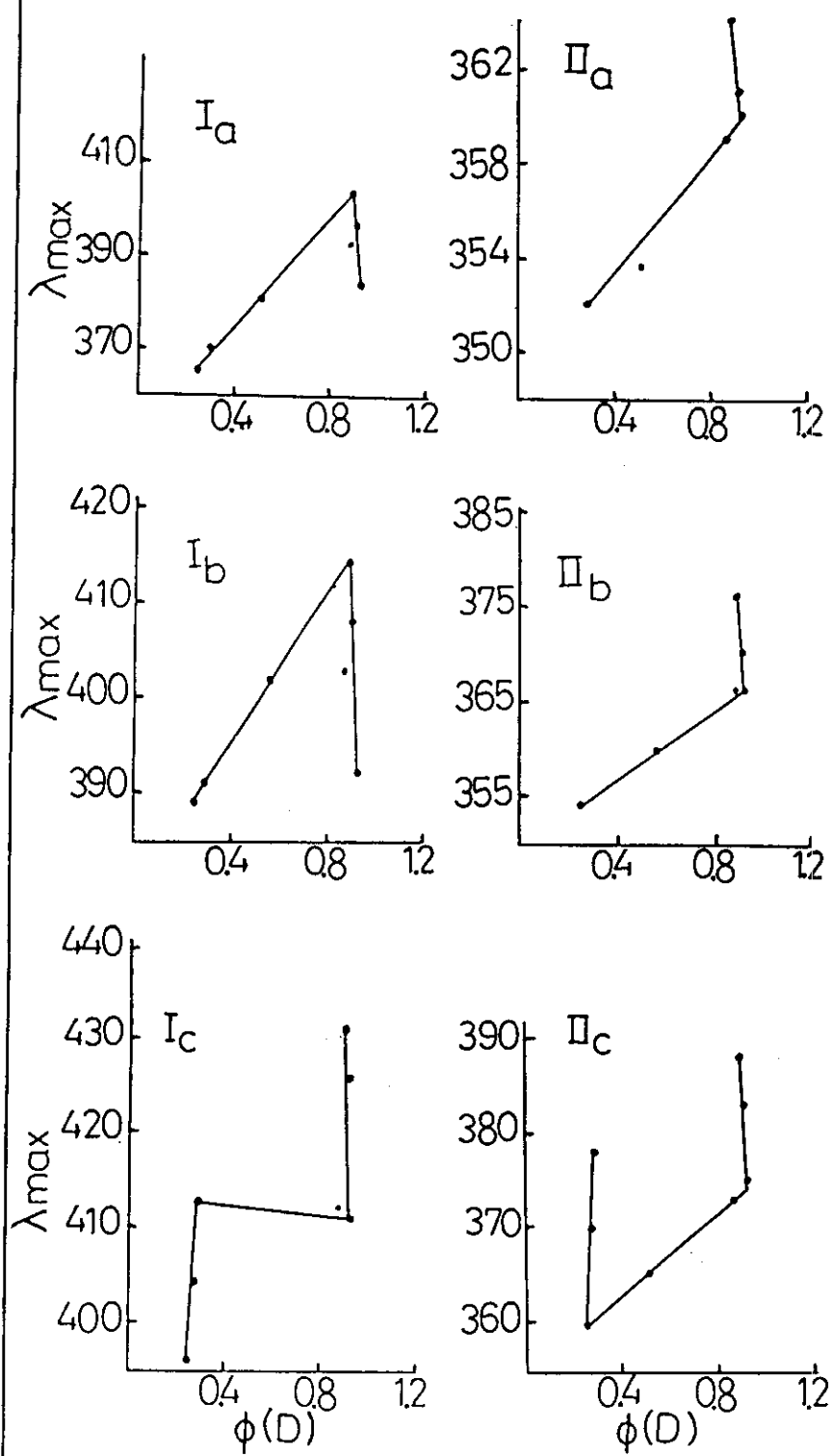


Fig. (9)

The Relation Between λ_{\max} And $\phi(D)$
Values For CT Band of Bis-Azo-
Compounds

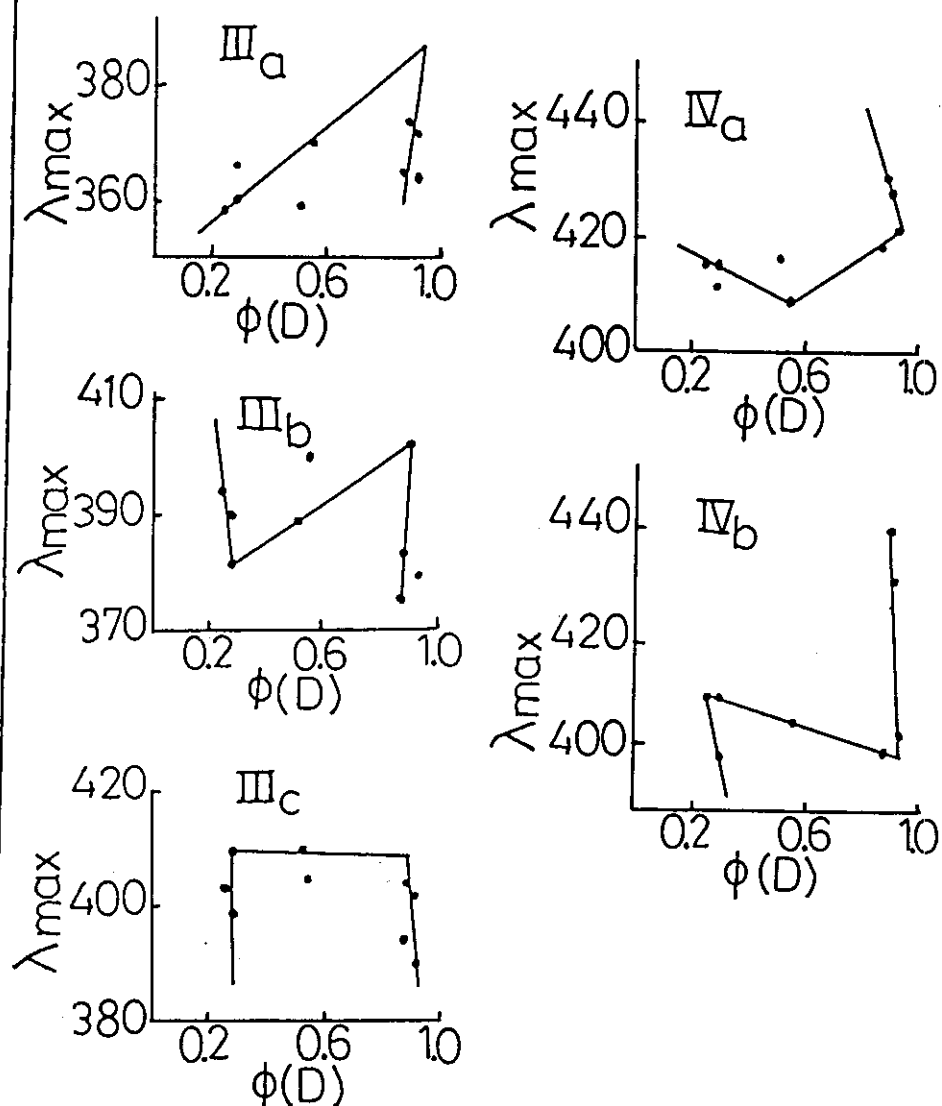


Fig.(10)

The Relation Between $\Delta\bar{\nu}$ And $f(n)$ Values For
CT Band of Mono-Azo-Compounds

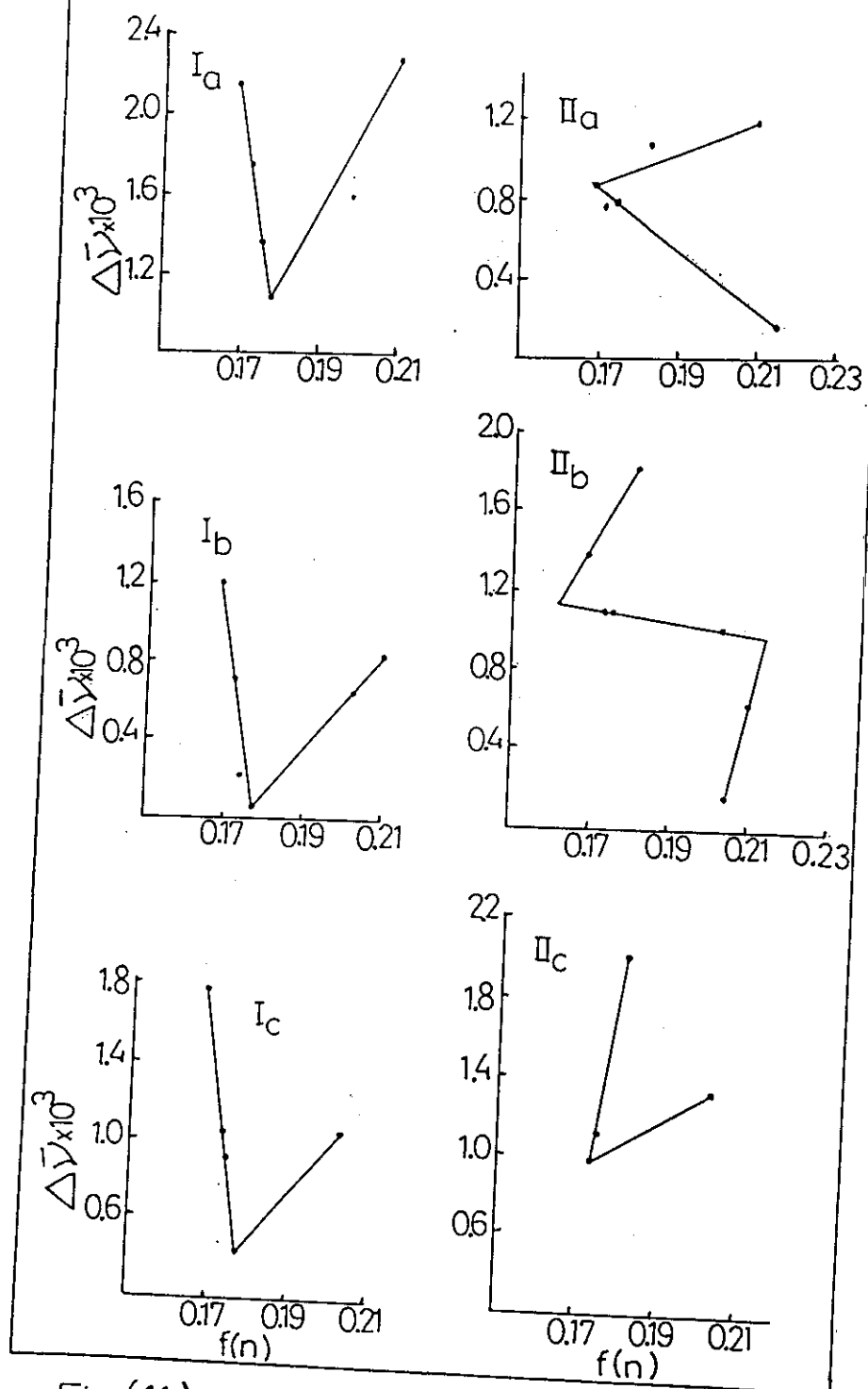


Fig.(11)

The Relation Between $\Delta\bar{\nu}$ And $f(n)$ Values For CT Band of

Bis-Azo-Compounds

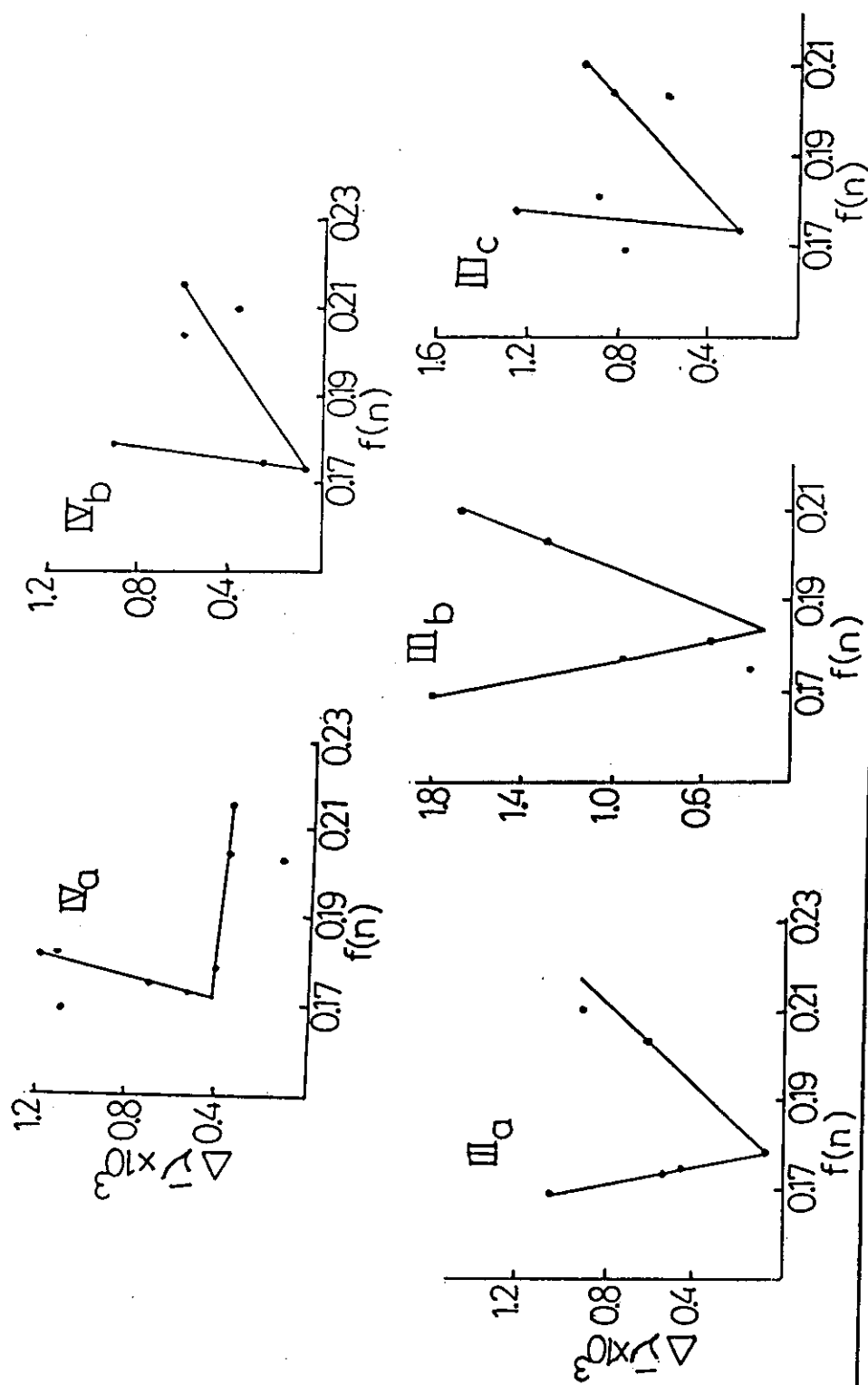


Fig.(12)

The Relation Between λ_{\max} And $f_2(n)$
Values For CT Band of Mono-Azo-
Compounds

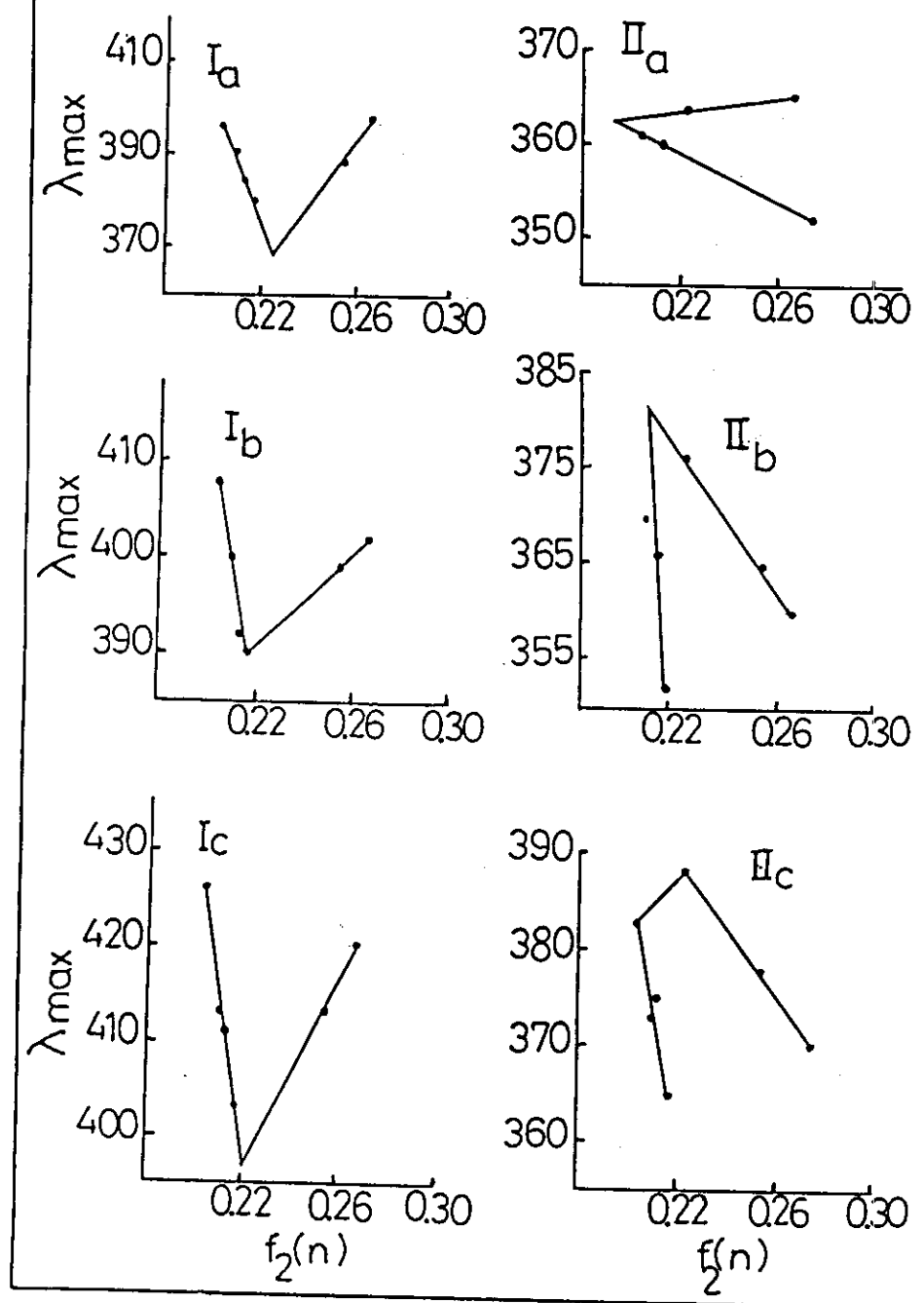


Fig.(13)

The Relation Between λ_{\max} And
Z Values For CT Band of Mono-
Azo-Compounds

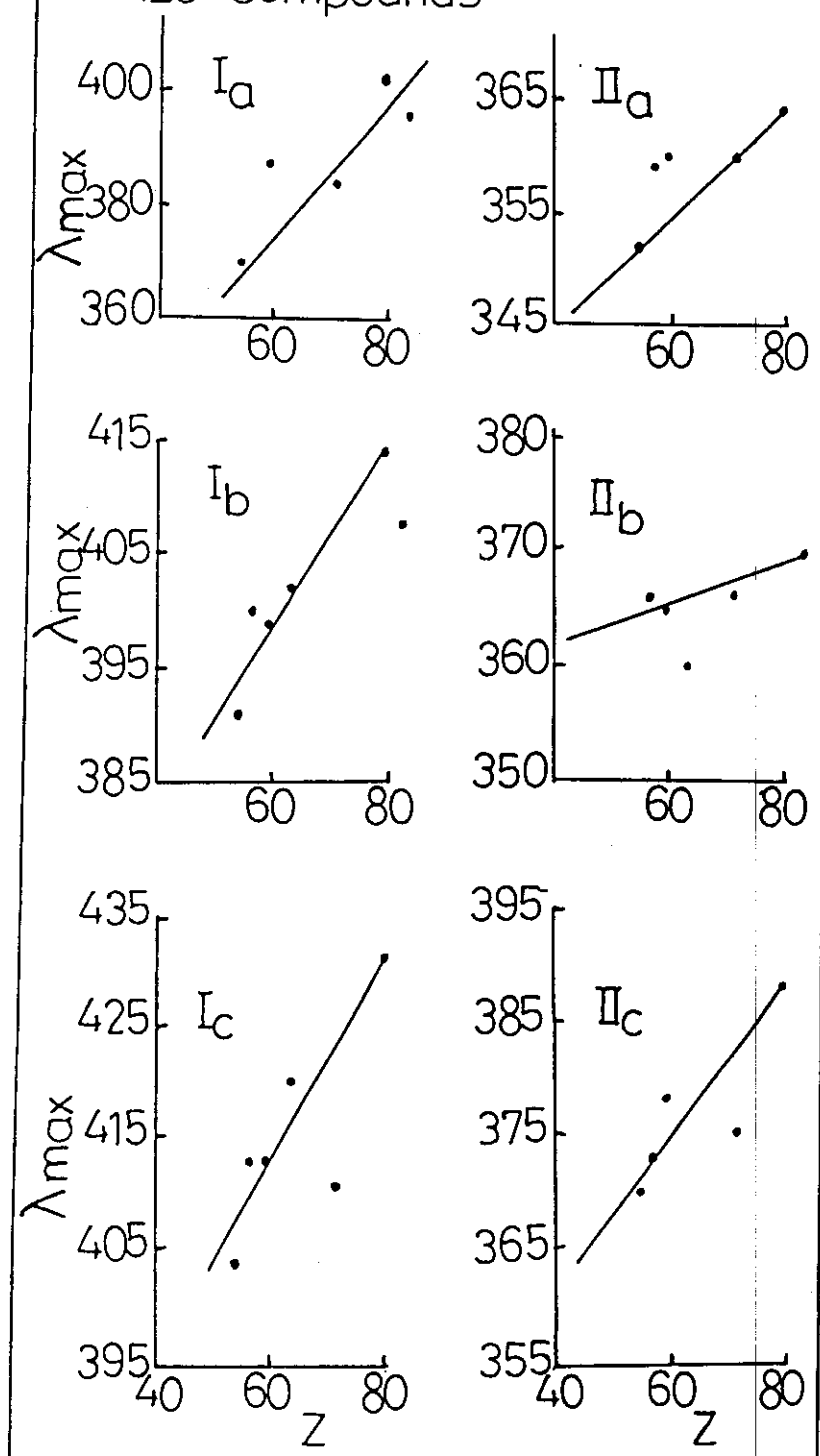


Fig. (15)

The Relation Between λ_{\max} And Z Values For CT Band of Bis-Azo-Compounds

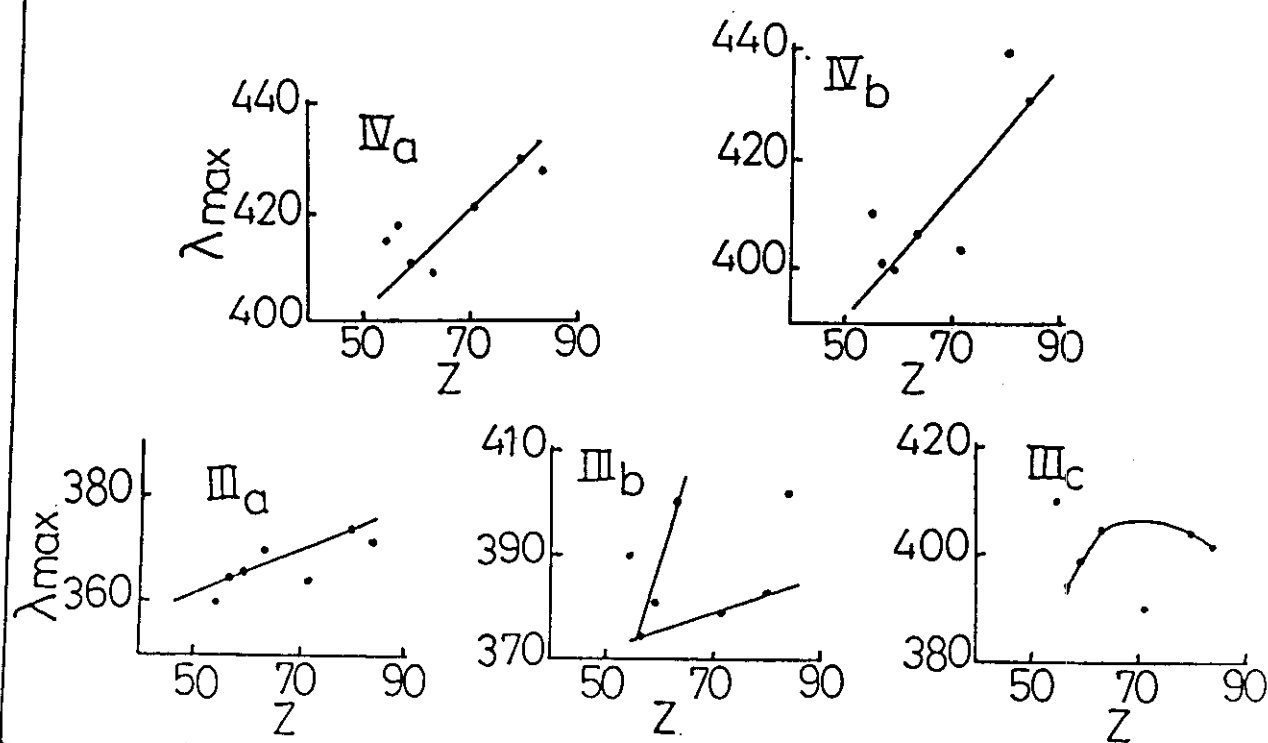


Fig. (16)

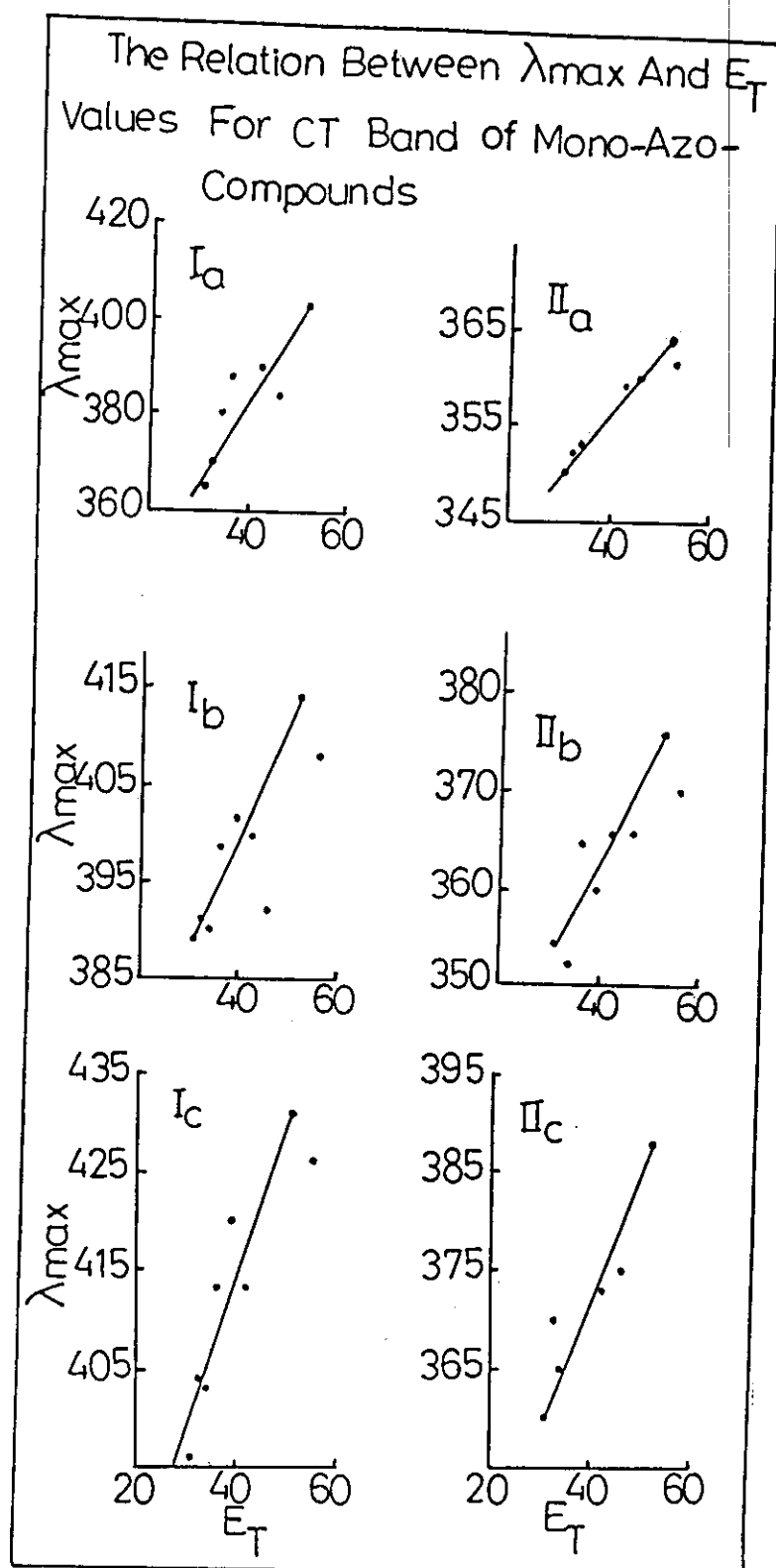


Fig. (17)

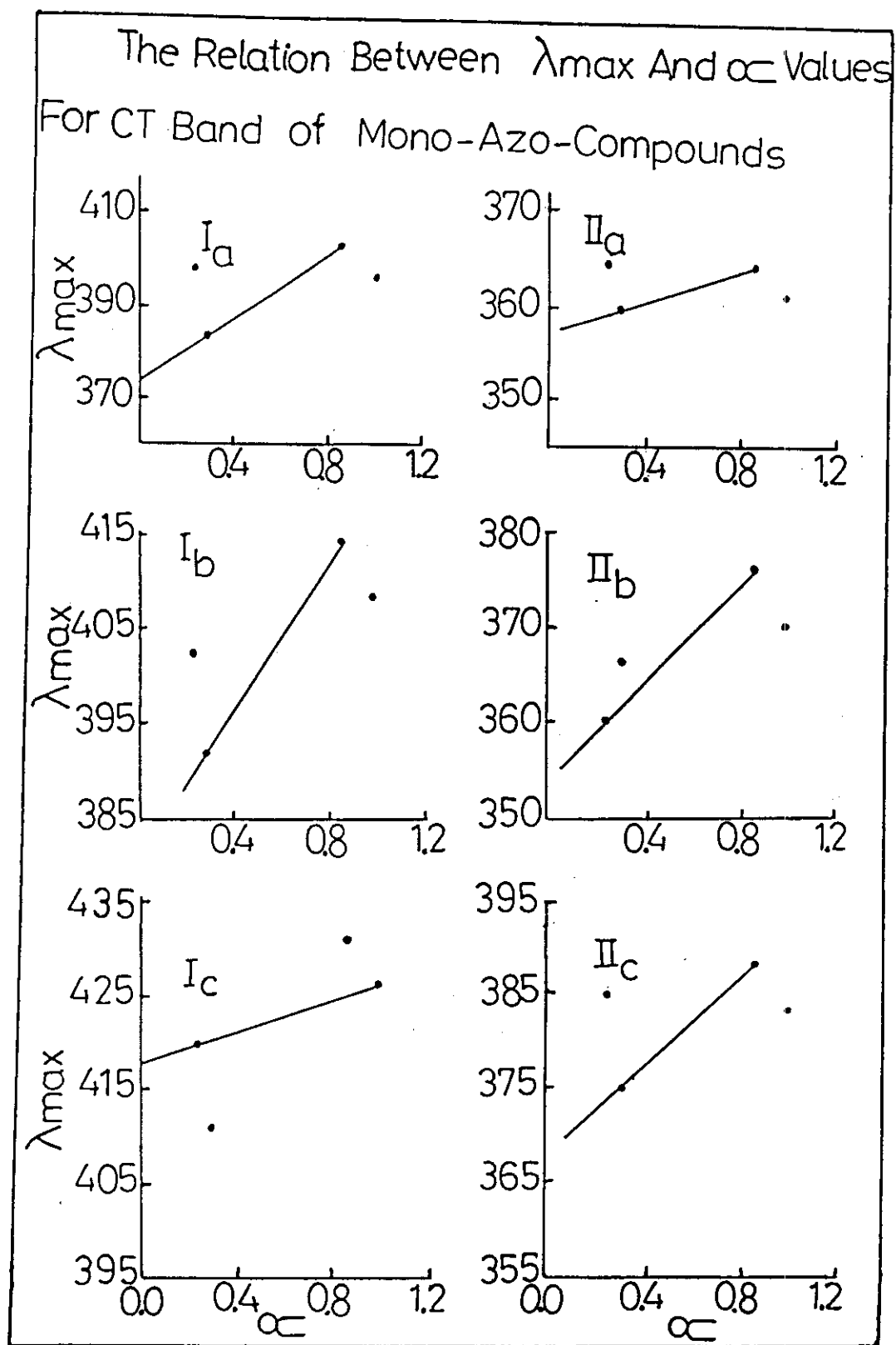


Fig. (19)

The Relation Between λ_{\max} And α Values For
CT Band of Bis-Azo-Compounds

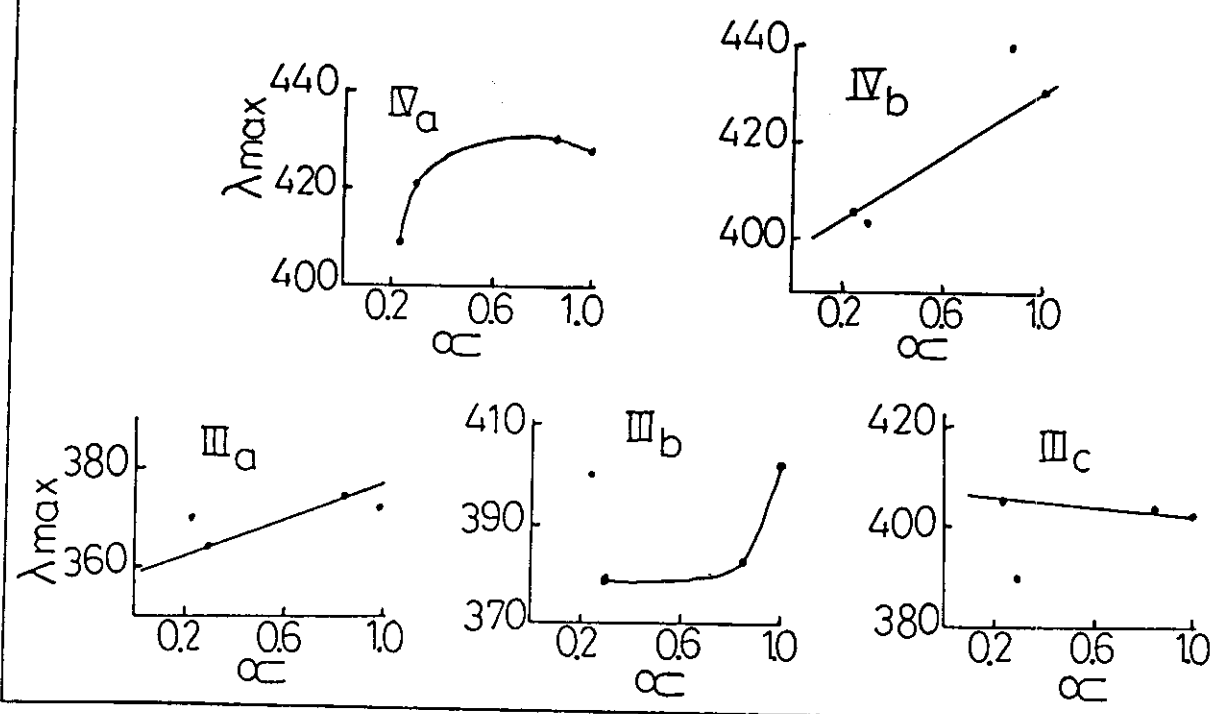


Fig.(20)

The Relation Between λ_{\max} And β Values For
CT Band of Bis-Azo-Compounds

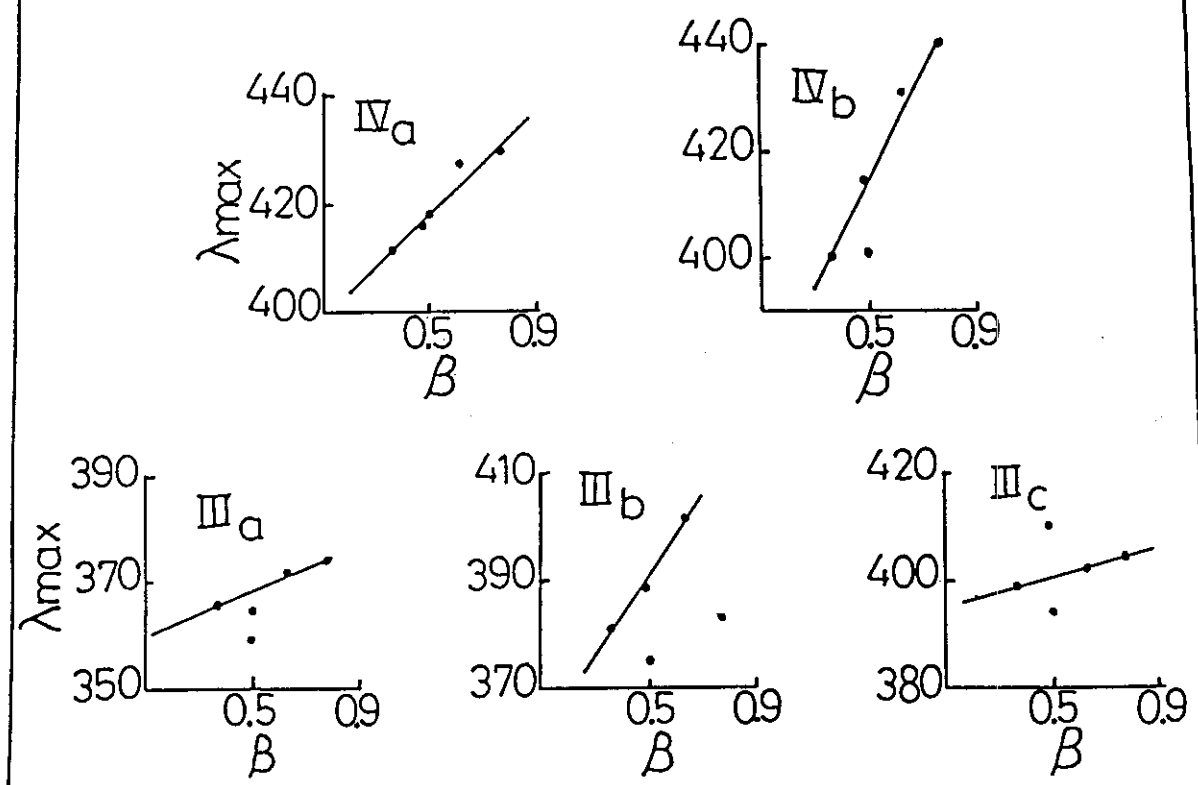


Fig.(22)

Spectral behaviour of some mono- and bis-azo- compounds in buffer solutions containing organic solvents and the determination of their acid ionisation constants:

The ionisation constants (pK_a) of some mono- and bis-azo-compound under investigation are determined spectrophotometrically in universal buffer solutions containing 30 % by volume of organic solvent. The absorption spectra of mono- and bis-azo-compounds in buffer solution of varying pH values are recorded within the wavelength range 200-600 nm. Thus the bands of some compounds were shifted in their position or show variation in extinction whereas others exhibit a new band by increasing pH of the medium.

Four different methods are applied for determination of pK_a of different compounds.

(1) Half- height method⁽⁷⁹⁾

The pK_a equal to the pH at half-height of the absorbance - pH curves.

(2) The modified limiting absorbance method⁽⁸⁰⁻⁸²⁾ :

This method has the advantage of eliminating any overlaps between absorbance of the two forms , and the pK_a is calculated by equation

$$pH = pK + \log \bar{\gamma} + \log \frac{A - A_{min}}{A_{max} - A}$$

where A = absorbance at a given pH value.

$\bar{\gamma}$ = is the activity coefficient of the ions present at equilibrium.

A_{min} , A_{max} are the absorbance corresponding to the total concentration of neutral and ionised species liable to exist in solution.

The pK_a value can be evaluated by plotting $\log \frac{A - A_{\min}}{A_{\max} - A}$ vs pH.

The pK_a value thus corresponds to the pH value at zero $\log \frac{A - A_{\min}}{A_{\max} - A}$.

(3) The colleter method⁽⁸³⁾

This method is utilised in the form developed for the determination of the stability constant of weak acids. The value of K can be calculated from equation.

$$K = \frac{C_{H_2^+} - M C_{H_3^+}}{M - 1}$$

$$\text{in which } M = \left(\frac{A_3 - A_1}{A_2 - A_1} \right) \cdot \left(\frac{C_{H_1^+} - C_{H_2^+}}{C_{H_1^+} - C_{H_3^+}} \right)$$

where A_1, A_2, A_3 are the absorbance at three different H^+ ion concentration $C_{H_1^+}, C_{H_2^+}$ and $C_{H_3^+}$ respectively.

(4) Modified isosbestic point^(84,85)

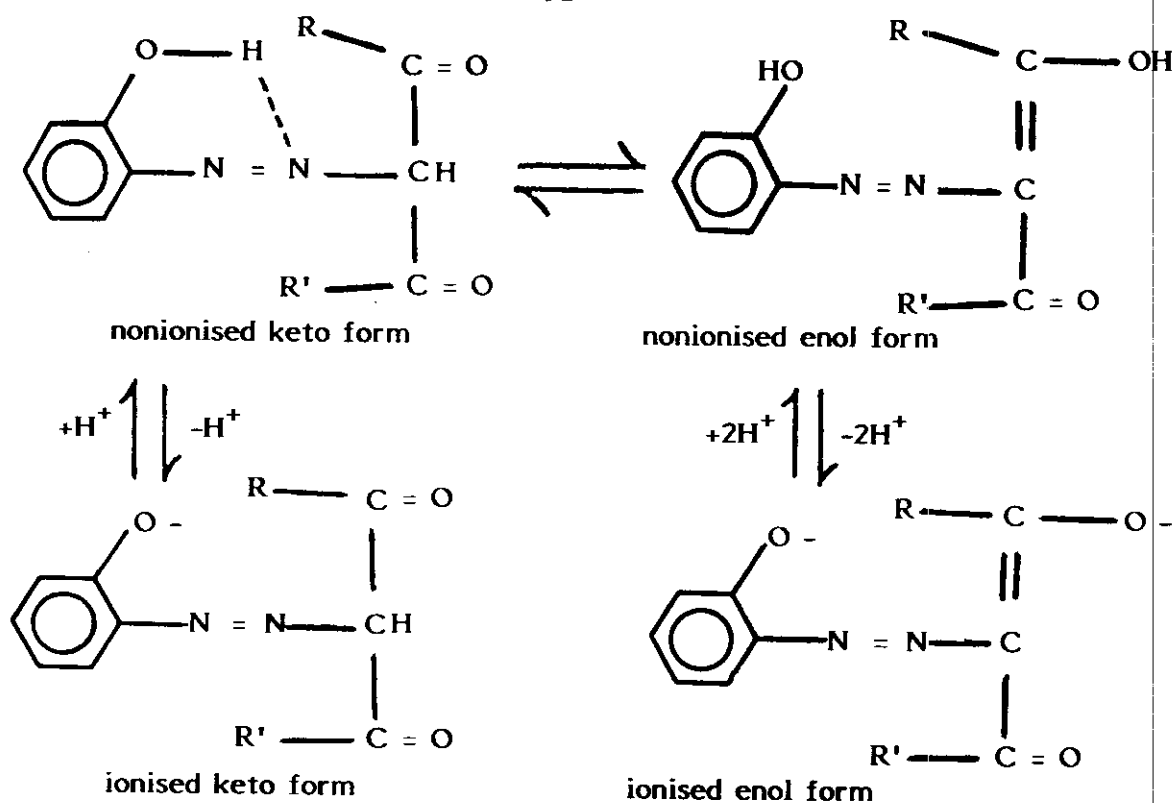
for acid - base equilibria



The following relation can be applied

$$pH = pK_a + \log \bar{\gamma} + \log \left(\frac{\epsilon_{R-O^-}}{\epsilon_{ROH}} \right) + \log \frac{(A - A_{\min}) RO^-}{(A - A_{\min}) ROH}$$

where ϵ_{R-OH} and ϵ_{RO^-} are the extinction coefficients of nonionised and ionised forms at λ_1 and λ_2 respectively. The correlation of $\log \frac{(A - A_{\min}) RO^-}{(A - A_{\min}) ROH}$ with pH yields linear relationship. The intercept of this line at $\log \frac{(A - A_{\min}) RO^-}{(A - A_{\min}) ROH}$ equals zero gives a value equivalent to the following



The average values of pK_a of azo compounds I_a , I_b and I_c calculated by the different four methods (Table 18) are 9.02, 8.57 and 8.00 respectively. Also the free energy change $-\Delta G^*$ ($\Delta G^* = -RT \ln K_a$) of I_a , I_b and I_c are equal to 12.26, 11.65 and 10.87 K. cal. mol^{-1} respectively.

Spectra of o-carboxyphenylazo- β -diketones II_a , II_b and II_c in buffer solutions:

The absorption spectra of 5×10^{-5} M of compounds II_a , II_b and II_c in universal buffer solutions containing 30 % EtOH by volume are shown in Figs (26-28). It is clear that the absorption of the species changes with increase of pH of the medium.

In case of II_a the absorbance of the visible band decreases in solutions of pH 1.89 to 4 then increased gradually with increasing the pH with small shifts in wavelength to red. This band was assigned as CT band

The variation of absorbance with pH of solution for compounds II_a, II_b and II_c are given in Figs. (26-28) as S- shape with one inflection. The pK_a values of the COOH and OH groups are determined using the three different methods (Tables 10-12). The mean pK_{a1} values for compounds II_a, II_b and II_c equal to 4.79, 4.16 and 3.37 and that of pK_{a2} are 10.4, 9.92 and 7.33 respectively.

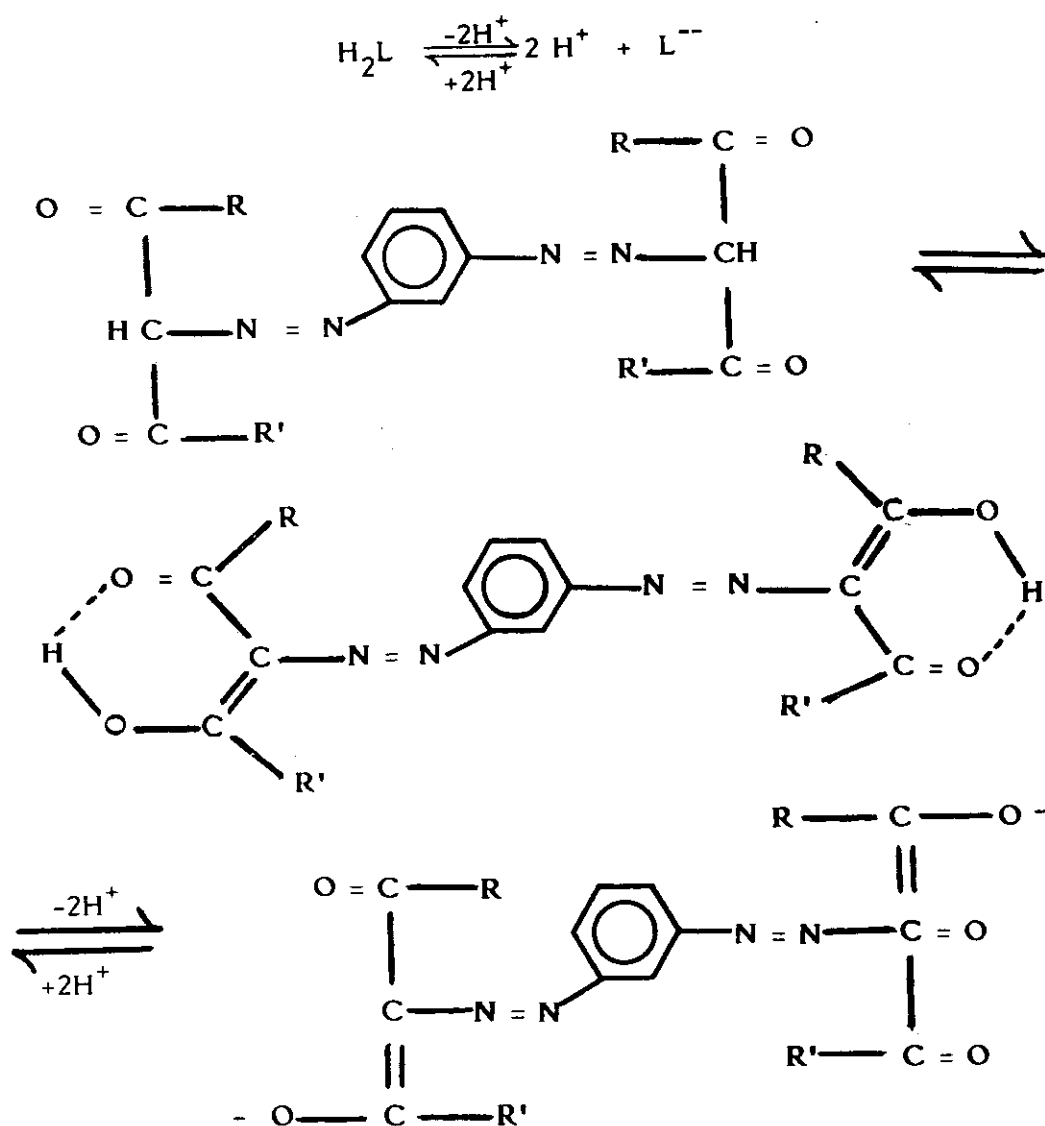
Spectra of m-bis-azobenzene-di-(β - diketones) III_a, III_b and III_c in mixed buffer solutions :

The absorption spectra of 5×10^{-5} M of the compounds III_a, III_b and III_c in buffer solutions containing 30 % dioxane by volume are recorded within the wavelength range 300-600 nm and shown in Figs. (29-31) . The spectra of the bis-azo dyes indicate that the nature of the absorbing species changes with pH. In case of III_a the curve shows that the bands at shorter and longer wavelength exhibit variation in extinction and position with pH. For first broadened band, which is a composite one comprising two peaks with λ_{\max} 365, 390 nm, the absorbance increases slightly with increasing the pH value of solution until 5.01. Above pH = 5.01 the extinction of the band decreases. At the same time the second peak of the first band disappears in solution of higher pH or in alkaline media whereas that of the first peak shifts to shorter wavelength. The second band at $\lambda_{\max} \approx 500$ nm exhibits slight variation in absorbance with pH. This behaviour is attributed to the strong intramolecular hydrogen bond between enolic OH group and the second carbonyl oxygen of the diketones.

In case of III_b the composite band at short wavelength exhibit variation

in absorbance with the pH of the medium which is not large as that of III_a . This behaviour indicate a strong H-bond of the enolic OH as in III_a .

In case of III_c the increase of pH of the medium causes a decrease in extinction of the two peaks of the first broaded band until pH 7.27. Above this pH the absorbance of the band increases. Also the longer wavelength band shows slight variation with pH. For compounds III_a , III_b and III_c the species liable to exist in solution is the neutral form and charged anions i.e. an acid-base equilibrium represented as :



The variation of absorbance with pH gives S- shaped curves as shown in Figs. (29-31) and the data are given in Tables (13-15). Three methods are used for calculation of pK_a values for compounds III_a , III_b and III_c which are found to be equal to 10.97, 8.47 and 7.57 respectively as shown in Table (18).

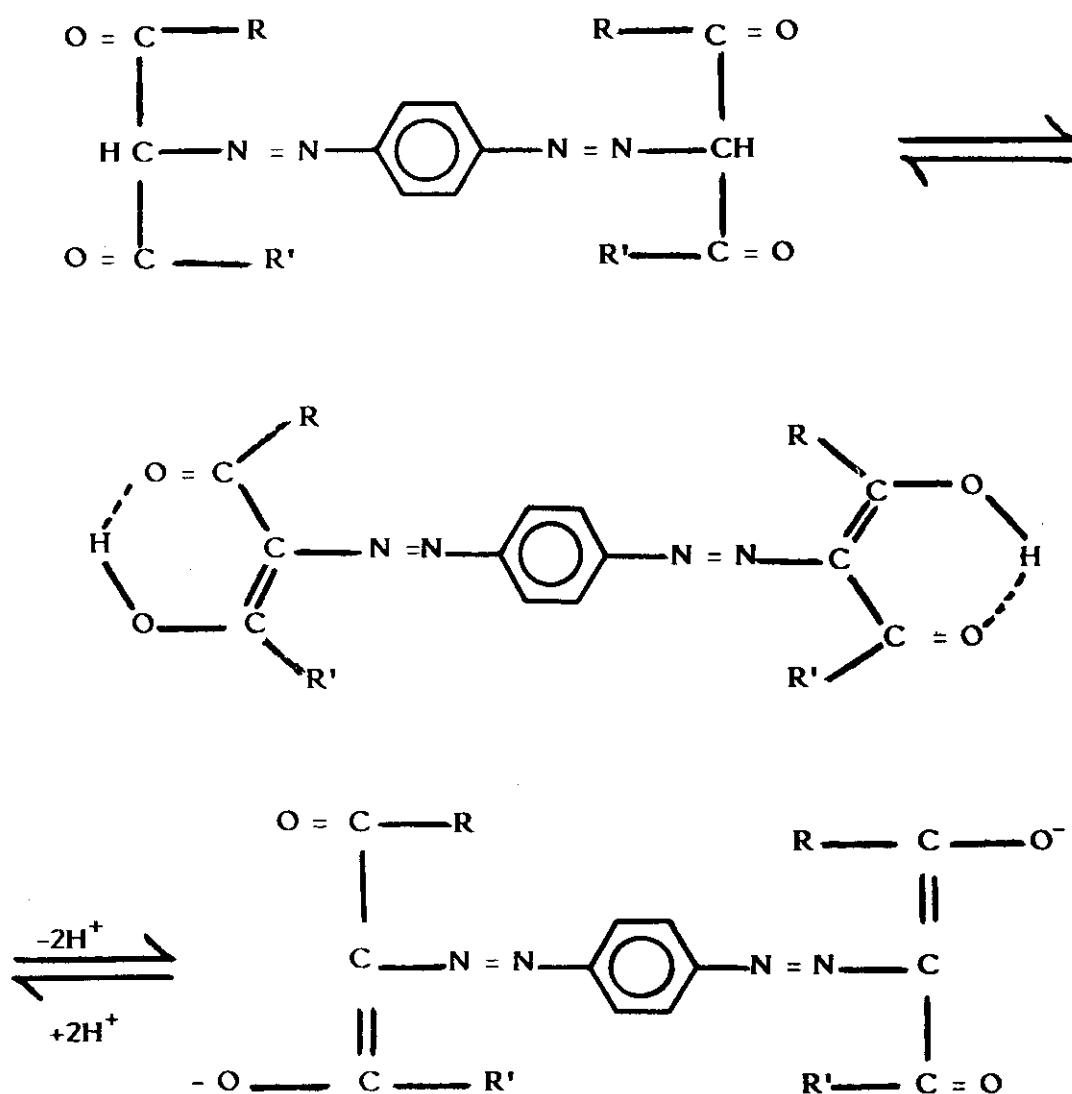
Spectra of p-bis-azobenzene-di(β -diketones) IV_a and IV_b in mixed buffer solutions :

The absorption spectra of 5×10^{-5} M of compounds IV_a , IV_b in mixed buffer solutions containing 30 % dioxane (V/V) are shown in Figs. (32,33). From the spectral curves, it is clear that the absorption of the species changes with pH of the solution. The spectra of IV_a show a band with $\lambda_{max} = 430$ nm in acidic solutions or that of lower pH values (1.89-5.01). At $pH > 7.27$ the band shifts to shorter wavelength ($\lambda_{max} \approx 380$ nm) with a decrease in extinction. The strong blue shift of the band is attributed to ionization of the compounds and the increase of the pH of the solution increases the percentage of the ionic species till at high pH where a very broad and low extinction band would appear. Thus the band at 430 nm is due to nonionised species, whereas that at 380 nm may due to ionised species. This behaviour can be attributed to the difference in the transition energy of the ionised formed and the nonionised one .

In case of IV_b the spectra exhibit a band at 415 nm the extinction of which increases with increasing pH till $pH = 7.27$, above which the absorbance of the band decreases with shift to shorter wavelength ($\lambda_{max} = 395$ nm). Another band appears with $\lambda_{max} = 325$ nm by increasing pH of the medium. The appearance of the last band indicates the presence

of the ionic species in equilibrium with the nonionic one. This was confirmed by the appearance of an isosbestic point at 360 nm.

The acid-base equilibrium can be represented as follows :



The variation of the absorbance with pH at different wavelengths gives S- shaped plots for IV_a, IV_b as shown in Figs. (32,33) and data are given in Tables (16,17). Three methods are used for calculation of pK_a values. The mean pK_a values of compounds IV_a and IV_b are equal to 11.43 and 9.66 respectively as shown in Table (18).

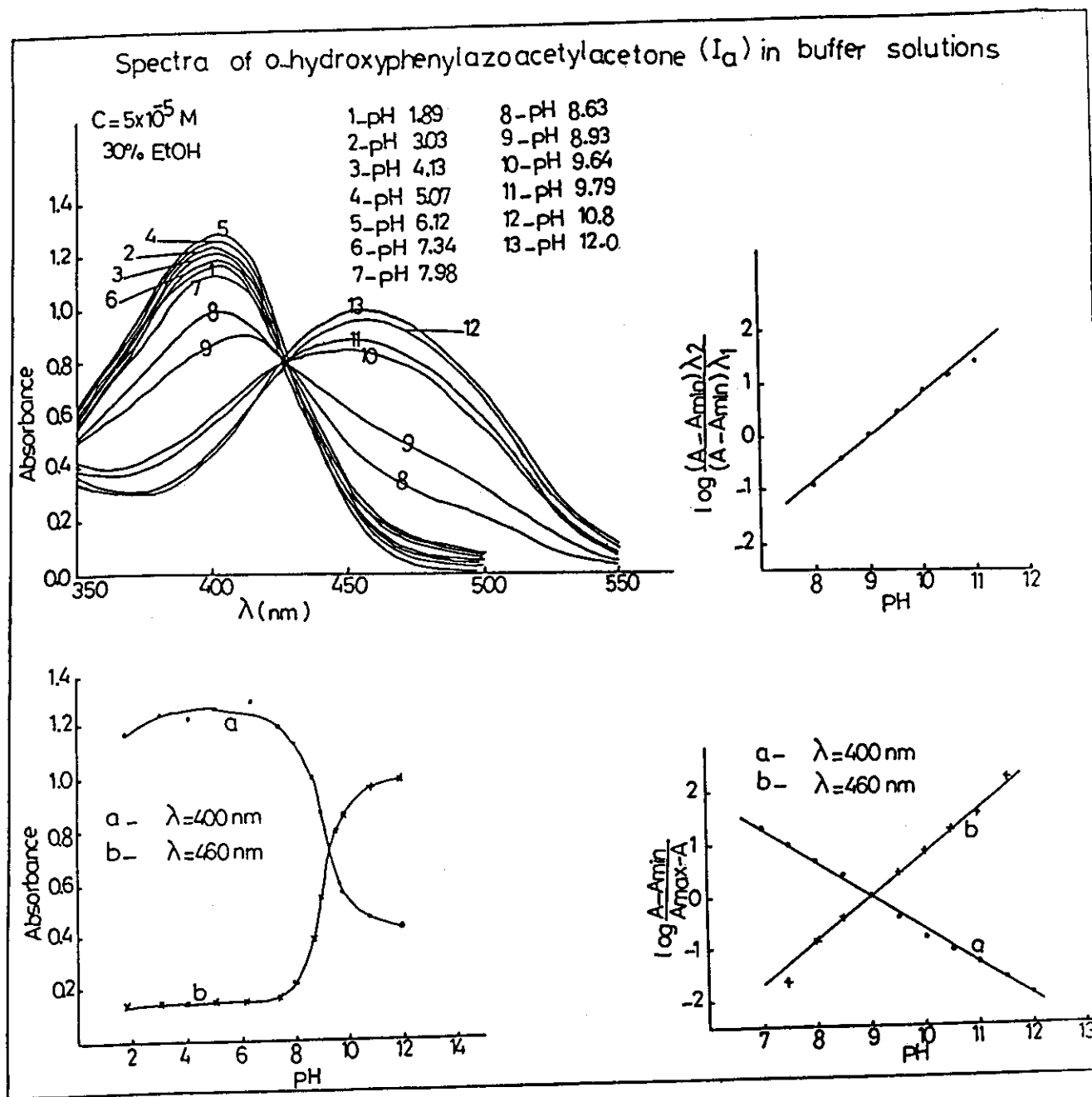


Fig. (23)

Table (7a) : The colleter method of compound I_a at $\lambda = 400$ nm

[illegible]

Table (7b) : The collector method of compound I_a at $\lambda = 460$ nm

points	pH	A	points taken	M	K_a	pK_a
1	7.5	0.155	2,3,4	1.8994	1.4041×10^{-9}	8.85
2	8.0	0.22	3,4,5	1.4435	1.2255×10^{-9}	8.91
3	8.5	0.36	4,5,6	1.2384	8.06996×10^{-10}	9.09
4	9.0	0.57	5,6,7	1.1396	4.5819×10^{-10}	9.34
5	9.5	0.76	6,7,8	1.0788	2.644×10^{-10}	9.58
6	10.0	0.88	1,5,9	1.3564	8.7525×10^{-10}	9.06
7	10.5	0.94	2,3,5	2.7256	1.3331×10^{-9}	8.88
8	11.0	0.965	2,4,8	1.9189	1.0674×10^{-9}	8.97
9	11.5	0.985	1,7,9	1.0590	4.7922×10^{-10}	9.32

mean $pK_a = 9.11$

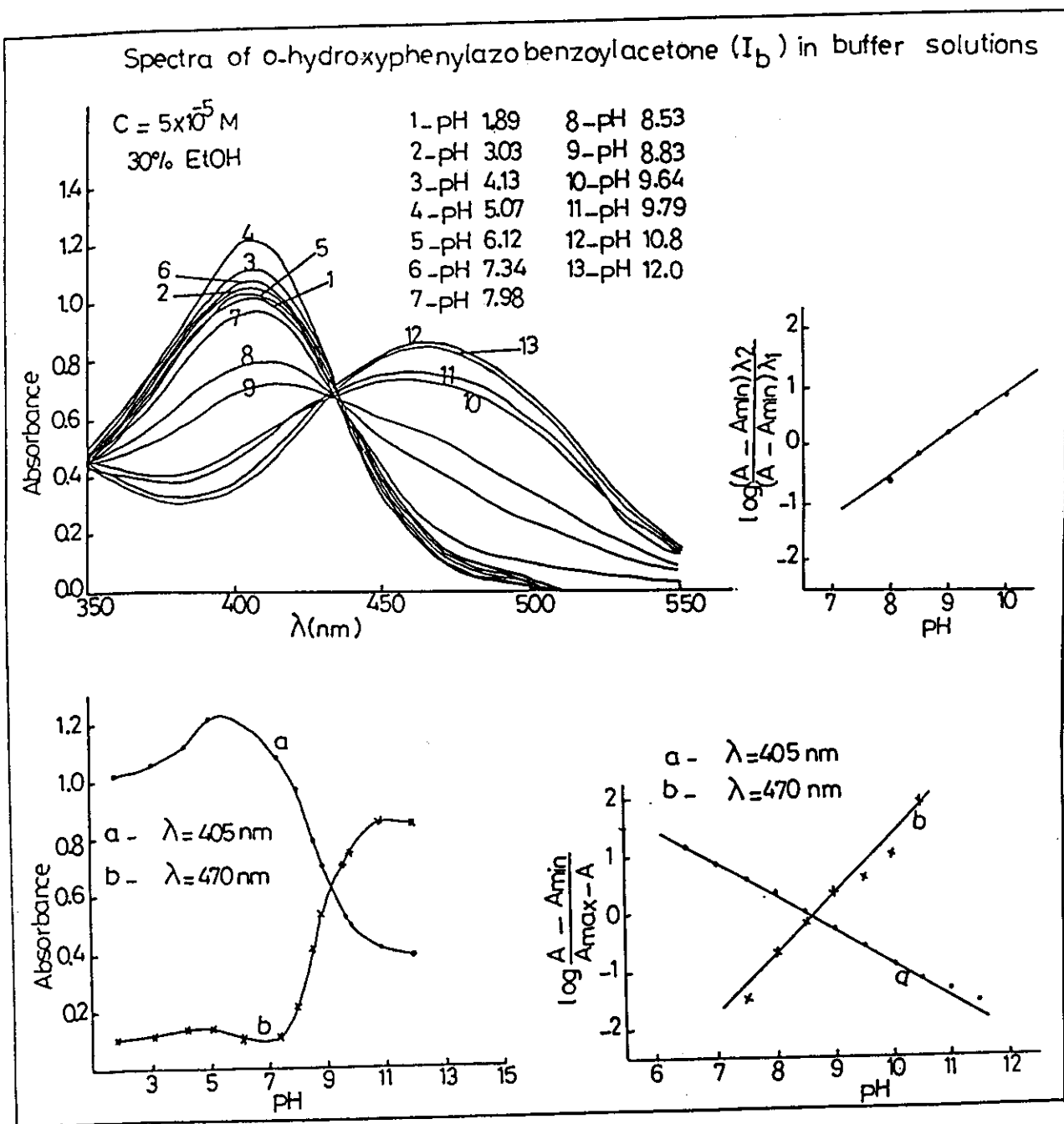


Fig.(24)

Table (8a) : The collector method of compound I_b at $\lambda = 405 \text{ nm}$

[illegible]

Table (8b) : The collector method of compound I_b at $\lambda = 470$ nm.

[illegible]

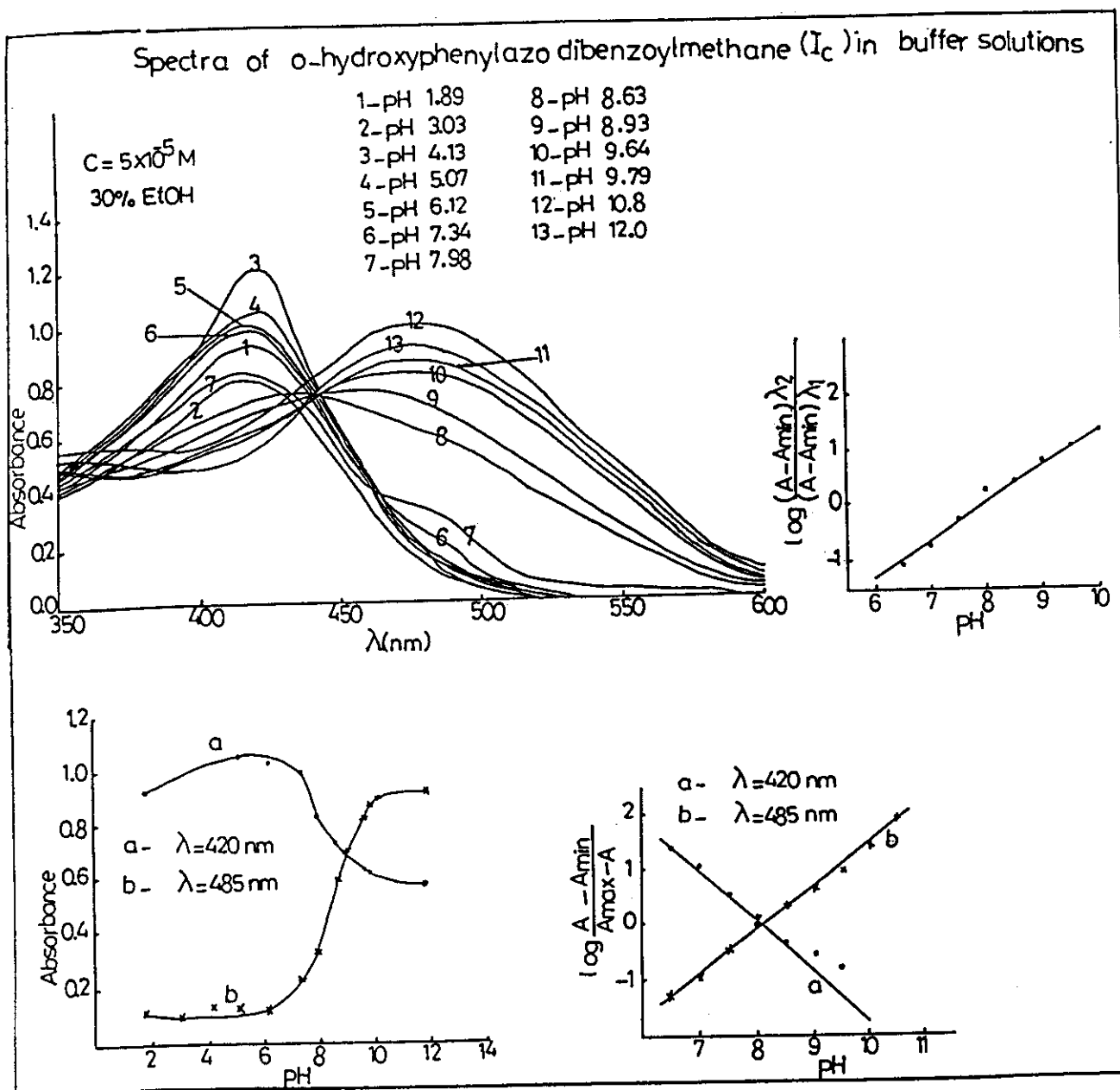


Fig.(25)

Table (9a) : The collector method of compound I_c at $\lambda = 420$ nm.

point s	pH	A	points taken	M	K_a	pK_a
1	6.5	1.04	1,2,3	3.4189	—	—
2	7.0	1.02	1,3,5	3.2364	9.56375×10^{-9}	8.01
3	7.5	0.95	3,4,5	1.1624	3.8942×10^{-8}	7.4
4	8.0	0.80	2,3,4	2.3856	5.6054×10^{-9}	8.25
5	8.5	0.72	2,6,9	1.2181	4.4084×10^{-9}	8.35
6	9.0	0.67	4,5,8	1.7267	4.11395×10^{-9}	8.38
7	9.5	0.63	1,6,9	1.2163	4.4454×10^{-9}	8.35
8	10.0	0.6	2,4,7	1.6071	1.5635×10^{-8}	7.8
9	10.5	0.59	3,5,6	1.1339	1.51485×10^{-8}	7.81

mean $pK_a = 8.04$

Table (9b): The collector method of compound I_c at $\lambda = 485$ nm.

[illegible]

Table (10a) : The collector method of compound II_a at $\lambda = 370$ nm

points	pH	A	points taken	M	K_{a_1}	pK_{a_1}
1	3.5	0.962	2,3,4	1.4967	3.3533×10^{-5}	4.47
2	4.0	0.988	3,4,5	1.3372	1.7116×10^{-5}	4.77
3	4.5	1.022	4,5,6	1.1852	1.0675×10^{-5}	4.97
4	5.0	1.055	2,6,8	1.1892	4.6569×10^{-6}	5.33
5	5.5	1.08	2,7,9	1.0769	3.6694×10^{-6}	5.44
6	6.0	1.094	1,8,9	1.01	6.8061×10^{-6}	5.17
7	6.5	1.107	1,3,5	1.7909	3.2823×10^{-5}	4.48
8	7.0	1.115	2,4,8	1.7117	1.381×10^{-5}	4.86
9	7.5	1.117	1,6,9	1.1664	5.78795×10^{-6}	5.24

mean $pK_{a_1} = 4.97$

Table (10b) : The collector method of compound II_a at $\lambda = 370$ nm

[illegible]

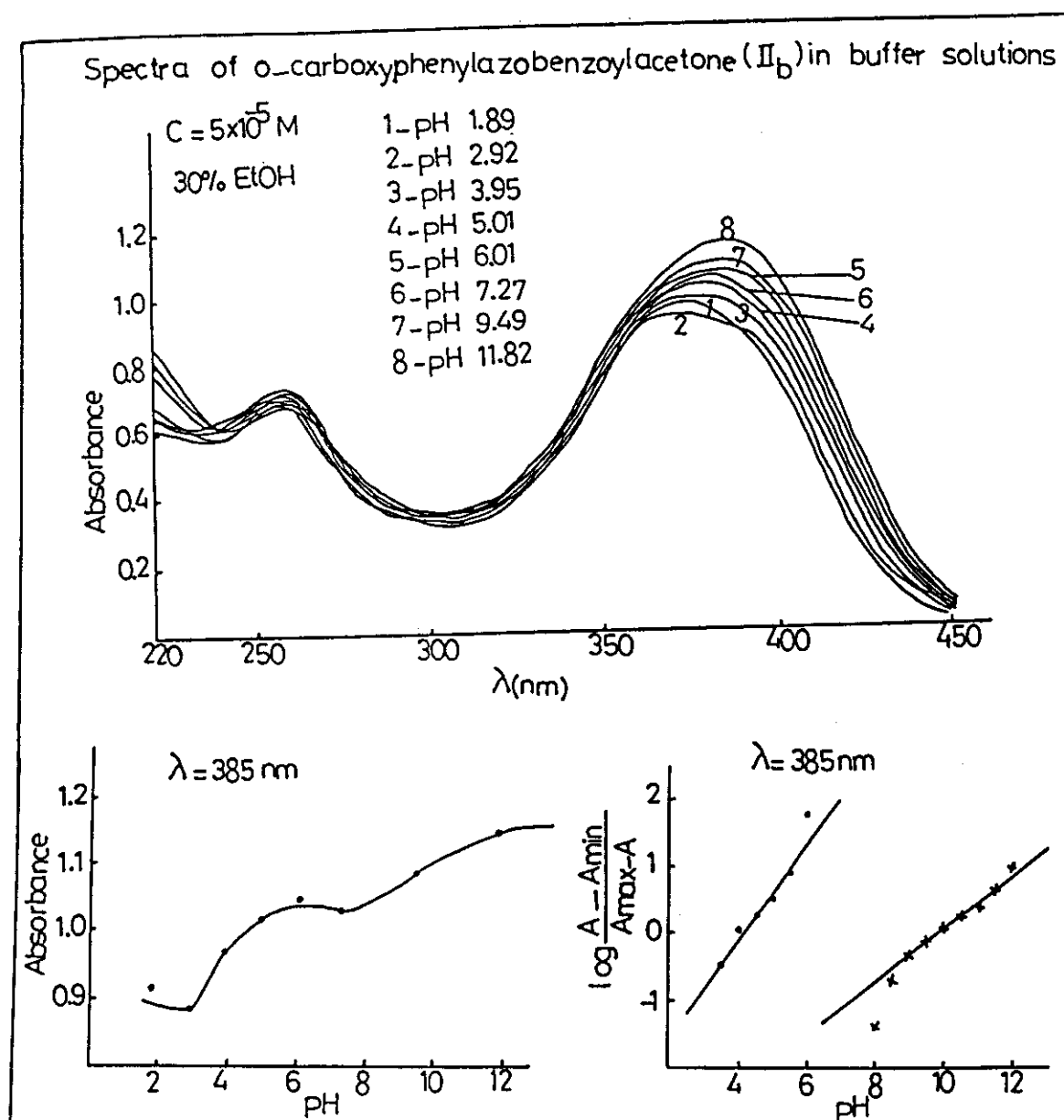


Fig.(27)

Table (11a) : The collector method of compound II_b $\lambda = 385$ nm

[illegible]

Table (11b) : The collector method of compound II_b at $\lambda = 385$ nm

points	pH	A	points taken	M	K_{a2}	pK_{a2}
1	8.0	1.035	2,3,4	1.37	1.5318×10^{-9}	8.81
2	8.5	1.05	3,4,5	1.43	4.0286×10^{-10}	9.39
3	9.0	1.07	4,5,6	1.30	1.9630×10^{-10}	9.71
4	9.5	1.086	5,6,7	1.52	3.1582×10^{-11}	10.5
5	10.0	1.1	1,7,8	1.18	3.4995×10^{-11}	10.46
6	10.5	1.11	1,3,7	2.19	8.2193×10^{-10}	9.09
7	11.0	1.12	2,6,8	1.41	6.6254×10^{-11}	10.18
8	11.5	1.135	5,7,8	1.63	7.6912×10^{-12}	11.11

mean $pK_{a2} = 9.91$

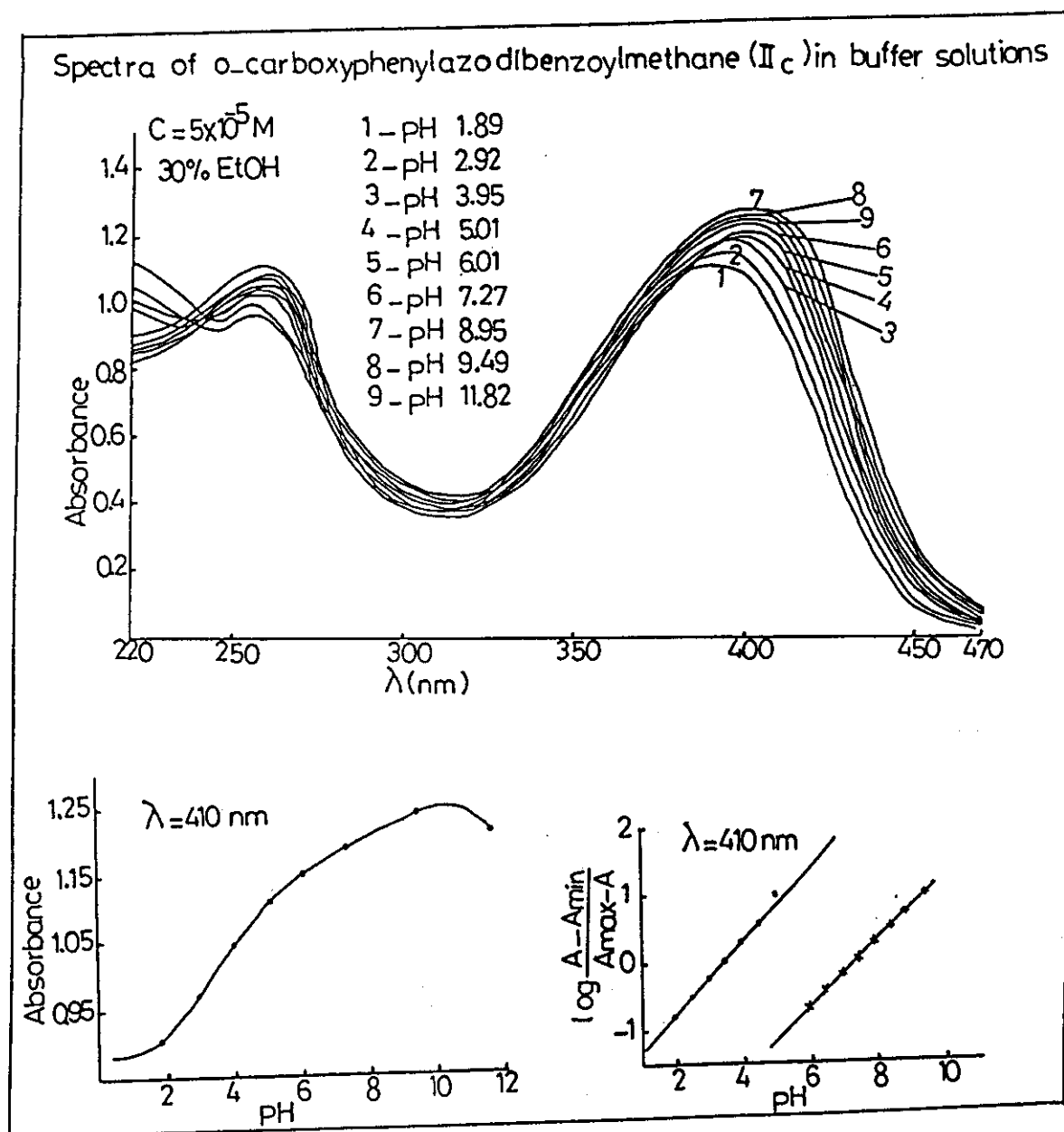


Fig.(28)

Table (12a) : The collector method of compound II_C at $\lambda = 410$ nm

points	pH	A	points taken	M	K_{a1}	pK_{a1}
1	2.0	0.915	1,2,3	1.6259	2.4547×10^{-3}	2.61
2	2.5	0.943	1,3,4	1.4684	1.1436×10^{-3}	2.94
3	3.0	0.975	2,3,4	1.5879	8.4685×10^{-4}	3.07
4	3.5	1.01	3,4,5	1.6259	2.45467×10^{-4}	3.61
5	4.0	1.05	2,4,5	1.4870	3.43995×10^{-4}	3.46
6	4.5	1.08	1,5,6	1.2116	2.9152×10^{-4}	3.54
7	5.0	1.11	2,6,7	1.2116	9.21870×10^{-5}	4.04

mean $pK_{a1} = 3.32$

Table (12b) : The collector method of compound II_C at $\lambda = 410 \text{ nm}$

points	pH	A	points taken	M	K_{a_2}	pK_{a_2}
1	6.0	1.15	1,2,3	1.5195	3.1622×10^{-7}	6.5
2	6.5	1.165	1,3,4	1.3941	1.41879×10^{-7}	6.85
3	7.0	1.18	2,3,4	1.5195	9.9998×10^{-8}	7.0
4	7.5	1.195	3,4,5	1.5195	3.1622×10^{-8}	7.5
5	8.0	1.21	2,4,5	1.3941	4.4866×10^{-8}	7.35
6	8.5	1.22	1,5,6	1.162	3.9046×10^{-8}	7.41
7	9.0	1.232	2,6,7	1.2116	9.2187×10^{-9}	8.04

mean $pK_{a_2} = 7.24$

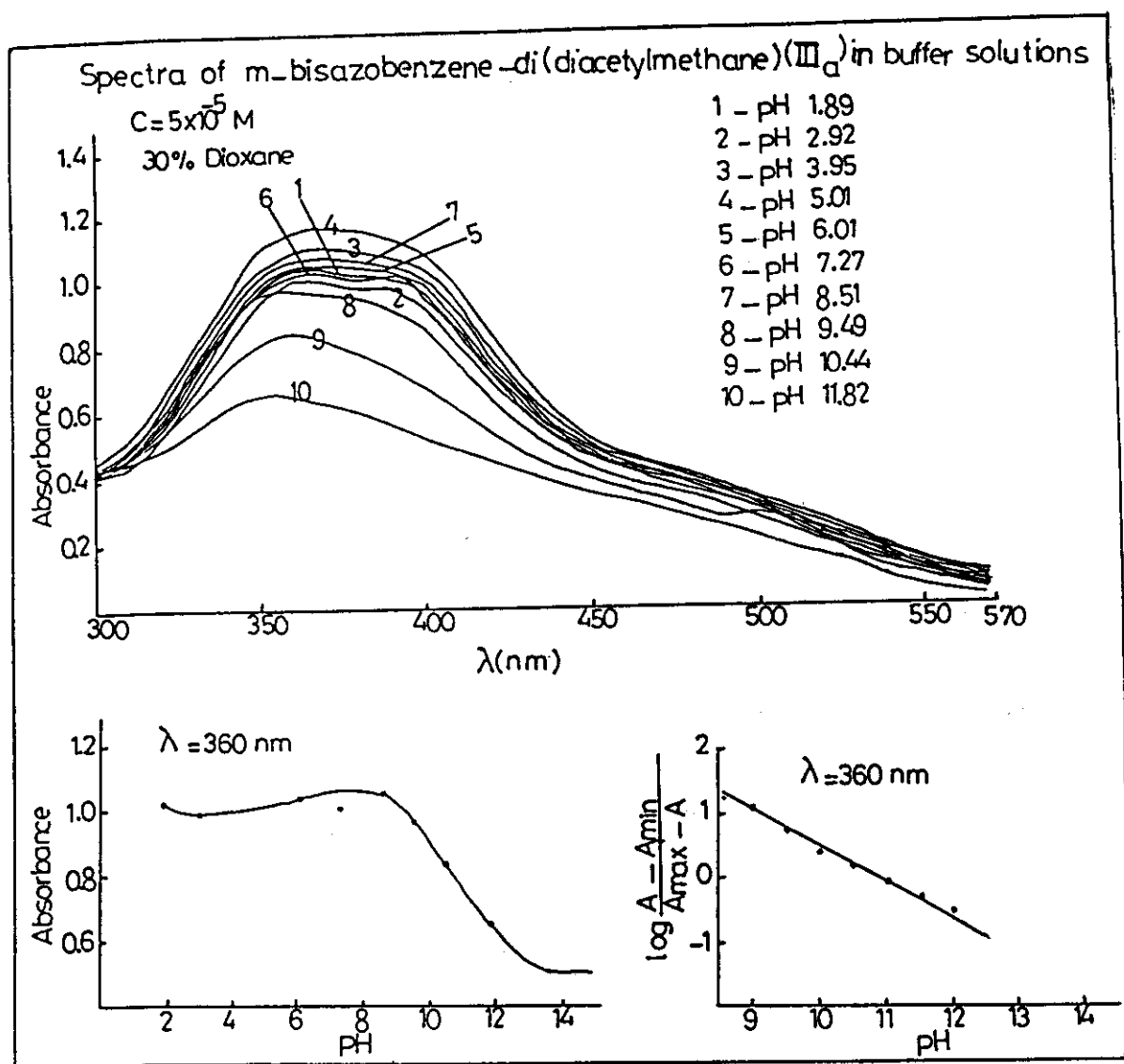


Fig.(29)

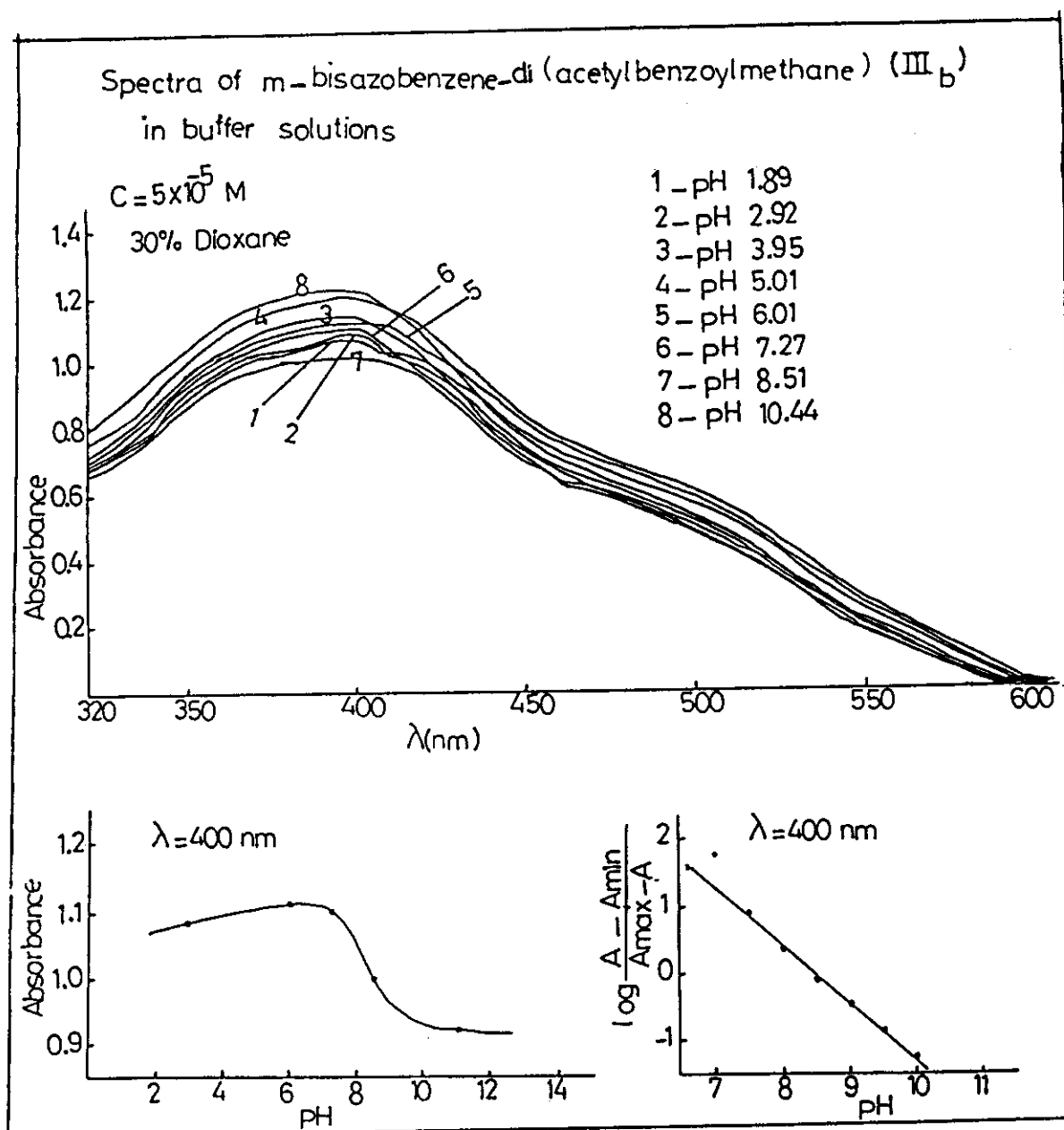


Fig. (30)

Table (13) : The collerter method of compound III_a at $\lambda = 360$ nm

points	pH	A	points taken	M	K_a	pK_a
1	9.0	1.02	2,3,4	1.52	9.9872×10^{-11}	10.0
2	9.5	0.97	3,4,5	1.52	3.1582×10^{-11}	10.5
3	10.0	0.9	4,5,6	1.52	9.9872×10^{-12}	11.0
4	10.5	0.83	5,6,7	1.41	4.2738×10^{-12}	11.37
5	11.0	0.76	2,7,8	1.19	3.2826×10^{-12}	11.48
6	11.5	0.69	7,8,9	1.109	1.8837×10^{-12}	11.72
7	12.0	0.63	1,8,9	1.07	2.989×10^{-12}	11.52

mean $pK_a = 11.08$

Table (14) : The collector method of compound III_b at $\lambda = 400$ nm

[illegible]

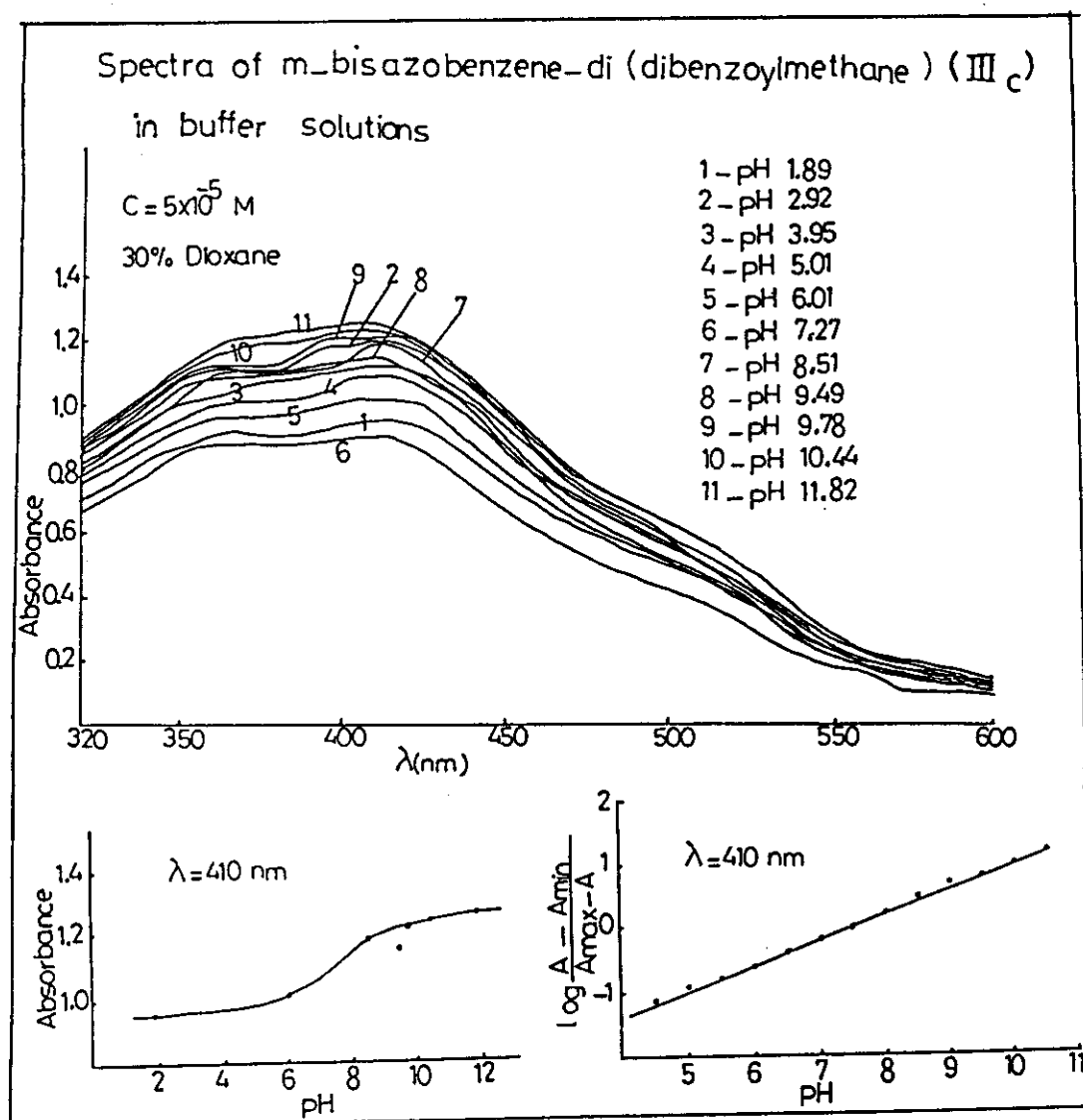


Fig.(31)

Table (15) : The collerter method of compound III_c at $\lambda = 410$ nm

points	pH	points taken	M	K _a	pK _a
1	4.5	6,8,10	1.7545	1.0928×10^{-8}	7.96
2	5.0	3,4,5	2.1843	2.61136×10^{-7}	6.58
3	5.5	4,5,6	1.5195	3.1622×10^{-7}	6.5
4	6.0	5,6,7	1.5195	9.9998×10^{-8}	7.0
5	6.5	6,7,8	1.7702	1.8074×10^{-8}	7.74
6	7.0	7,8,9	1.5195	9.9998×10^{-9}	8.0
7	7.5	8,9,10	1.2346	8.2169×10^{-9}	8.09
8	8.0	1,9,10	1.1199	1.7034×10^{-8}	7.77
9	8.5	2,3,10	1.271	2.6896×10^{-7}	6.57
10	9.0	1,3,9	8.51	4.1749×10^{-7}	6.38
11	9.5	9,11,12	1.2547	7.4895×10^{-10}	9.13
12	10.0	7,11,12	1.1024	2.0116×10^{-9}	8.7
mean pK _a = 7.54					

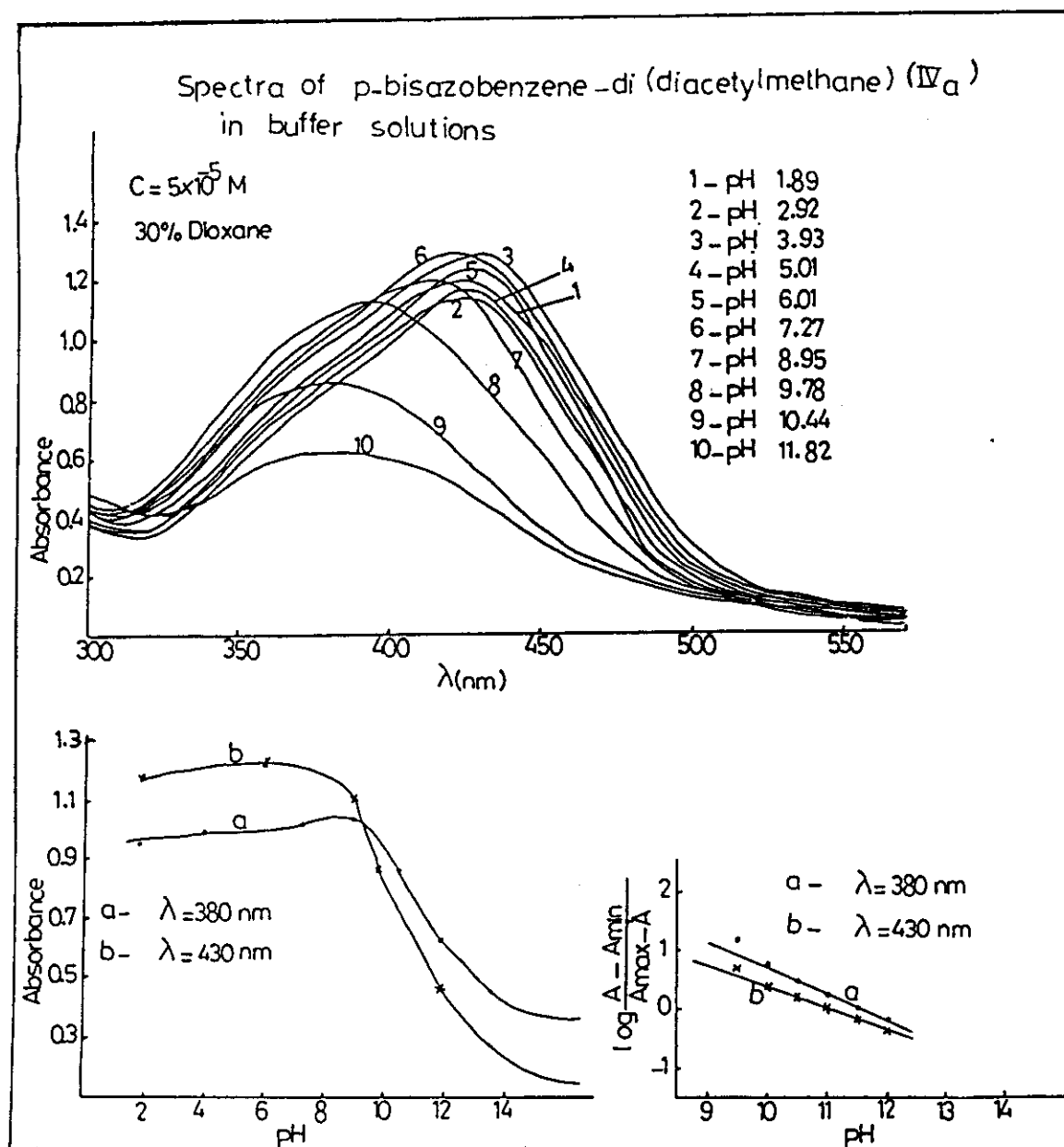


Fig.(32)

Table (16a) : The colleter method of compound IV_a at $\lambda = 380$ nm

points	pH	A	points taken	M	K_a	pK_a
1	9.5	1.0	2,3,4	1.5195	3.1622×10^{-11}	10.50
2	10.0	0.94	3,4,5	1.4739	1.1266×10^{-11}	11.0
3	10.5	0.855	4,5,6	1.4739	3.5627×10^{-12}	11.5
4	11.0	0.77	5,6,7	1.3675	1.5444×10^{-12}	11.81
5	11.5	0.69	6,7,8	1.4587	3.7139×10^{-13}	12.43
6	12.0	0.615	7,8,9	1.4511	1.1996×10^{-13}	12.92

mean $pK_a = 11.70$

Table (16b) : The collector method of compound IV_a at $\lambda = 430$ nm

points	pH	A	points taken	M	K_a	pK_a
1	9.5	0.96	2,3,4	1.4815	3.4907×10^{-11}	10.5
2	10.0	0.825	3,4,5	1.6487	7.3784×10^{-12}	11.13
3	10.5	0.73	4,5,6	1.4435	3.8755×10^{-12}	11.41
4	11.0	0.64	5,6,7	1.2384	2.5519×10^{-12}	11.6
5	11.5	0.535	6,7,8	1.5195	3.1622×10^{-13}	12.5
6	12.0	0.44	7,8,9	1.2688	2.2276×10^{-13}	12.7

mean $pK_a = 11.64$

Table (17b) : The collector method of compound IV_b at $\lambda = 415 \text{ nm}$.

[illegible]

Table (18) : The ionisation constants (pK_a) for mono- and bis-azo-compounds.

aqueous — solvent 30% V/V	compound	group	pK_a					$-\Delta G^*$ K.cal/M
			1	2	3	4	average	
EtOH	I _a	OH	9.0	9.0	9.07	9.0	9.02	12.26
EtOH	I _b	OH	8.55	8.55	8.51	8.66	8.57	11.65
EtOH	I _c	OH	7.96	8.04	8.06	7.95	8.00	10.87
EtOH	II _a	COOH	4.7	4.71	4.97	—	4.79	6.51
		OH	10.4	10.42	10.32	—	10.40	14.13
EtOH	II _b	COOH	4.0	4.15	4.32	—	4.16	5.65
		OH	9.9	9.95	9.91	—	9.92	13.48
EtOH	II _c	COOH	3.4	3.4	3.32	—	3.37	4.58
		OH	7.35	7.4	7.24	—	7.33	9.96
dioxane	III _a	OH	10.9	10.92	11.08	—	10.97	14.91
dioxane	III _b	OH	8.42	8.48	8.52	—	8.47	11.51
dioxane	III _c	OH	7.6	7.57	7.54	—	7.57	10.29
dioxane	IV _a	OH	11.24	11.35	11.70	—	11.43	15.53
dioxane	IV _b	OH	9.68	9.68	9.61	—	9.66	13.13

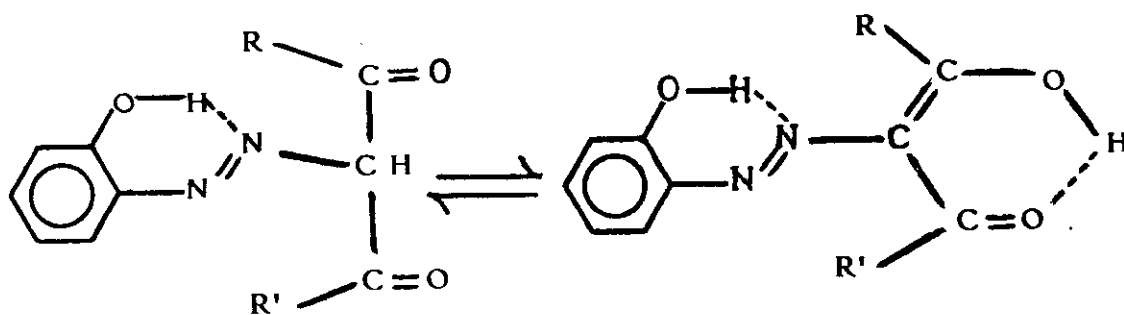
Infrared spectra of free mono- and bis- azo compounds :

This part includes an attempt to obtain the assignment for the important and characteristic bands in the ir- spectra of the azo dyes under investigation.

The ir- spectra of the azo compounds under investigation are recorded in Figs. (47-52, 76-80). The assignment of the important bands is given in Table (19) and interpreted in the light of molecular structure. The band assignment given in the present investigation is achieved by the comparison method and considering the effect of substitution and molecular structure on the position of different bands. The method is more or less similar to that applied in the case of some aromatic compounds⁽⁸⁶⁾ and azobenzenes⁽⁸⁷⁾. The new bands observed in the spectra of the dyes are due to the vibration of OH, COOH, CH₃, N=N, C=O groups, other substituted phenyl ring and the slight change of the symmetry of the molecule.

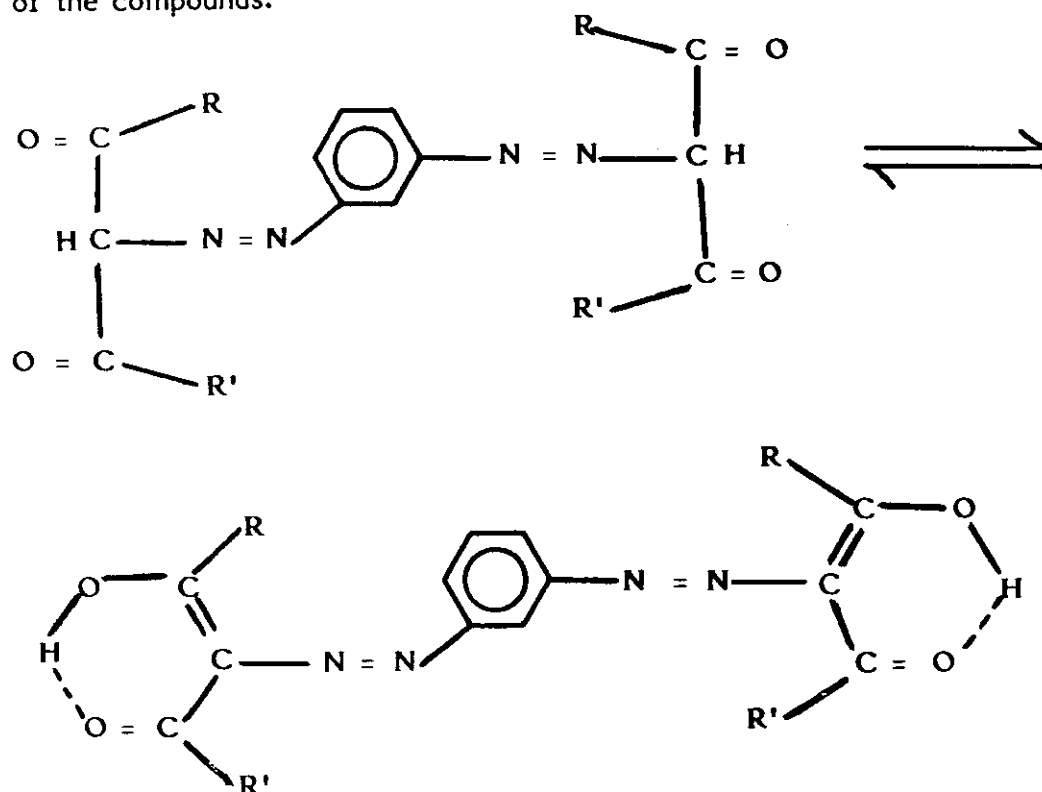
Spectra in the range 4000-2000 cm⁻¹ :

In this region the bands due to the OH, COOH, N-H and C-H stretching vibrations are expected to appear. For the first series of compounds (I), the ν_{OH} band appears as a wide broad absorption with medium intensity at lower frequency 3000, 3360, 3080 cm⁻¹ for I_a, I_b and I_c respectively. The position of these bands indicate that the OH group in the o-position of phenyl ring is contributing to an intramolecular H-bond with the second nitrogen atom of -N=N- group to form a six membered ring. Also the enolic OH group would form an intramolecular H-bond with the oxygen of carbonyl group.



The stretching vibration of OH of the carboxylic group in the second series II_{a-c} leads to a broad band at 3020, 3400 and 3130 cm^{-1} respectively, supporting its intramolecular H-bonding with the N=N group as well as the enolic OH with C=O group.

The ν_{OH} band of enolic form of the third series of compounds (III) appears as a broad weak intensity band at 3400, 3360 and 3060 cm^{-1} for III_a, III_b and III_c respectively. Also the position of such band indicates the intramolecular H-bond with the second C=O group of the diketone part of the compounds.



From the spectra of the compounds III_{a-c} Figs. (76-78) it is clear that a strong and very broadened band appeared at higher wavenumber, which is due to the stretching vibration of the OH of water molecules. The ν_{OH} band of enolic form of the fourth series of compounds IV appear at 3480 and 3440 cm^{-1} for IV_a and IV_b as a broad band.

The C-H stretching vibration of the CH₃ group for compounds I_{a,b}, II_{a,b}, III_{a,b} and IV_{a,b} is appear at the range 3030-2820 cm^{-1} .

ir- spectra in the range 2000-1500 cm^{-1} :

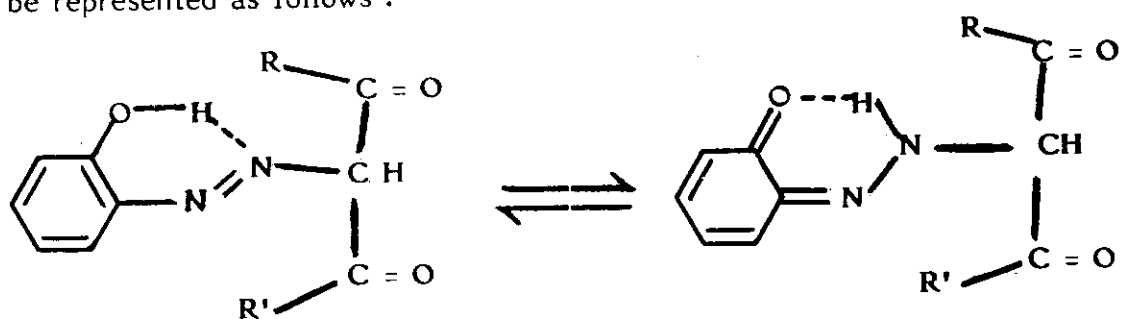
The bands due to the stretching vibrations of C=O, C=C and C=N deformation are expected to appear in this region. For the first series of compounds I_c, I_a and I_b the $\nu_{C=O}$ bands appeared at 1621, 1631 and 1646 cm^{-1} respectively and shows a shift to higher frequency in the order I_b > I_a > I_c. The $\nu_{C=C}$ band appears at 1599, 1620 and 1597 cm^{-1} for I_a, I_b and I_c respectively. The $\delta_{C=N}$ band for I_a, I_b and I_c appear at 1509, 1512 and 1517 cm^{-1} respectively.

For compounds of the second series (II), the $\nu_{C=O}$ bands are shown at 1700, 1641 and 1679 cm^{-1} for II_a, II_b and II_c respectively. The $\nu_{C=C}$ bands for II_a, II_b and II_c appear at 1635, 1622 and 1639 cm^{-1} respectively. The $\delta_{C=N}$ band is observed at 1578, 1582 and 1574 cm^{-1} for II_a, II_b and II_c respectively.

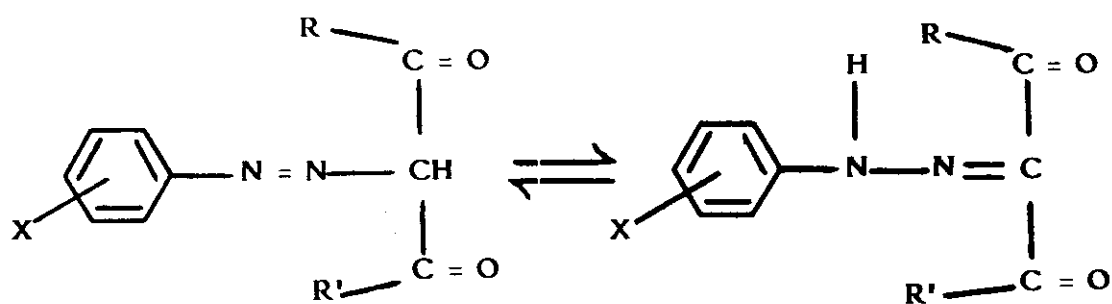
For the compounds of the third series (III), the $\nu_{C=O}$ band appear at 1648, 1675 and 1644 cm^{-1} for III_a, III_b and III_c. Also $\nu_{C=C}$ band at

1600, 1603 and 1598 cm^{-1} for III_a , III_b and III_c respectively. The $\delta_{\text{C=N}}$ band is also shown at 1510, 1509 and 1510 cm^{-1} for III_a , III_b and III_c respectively.

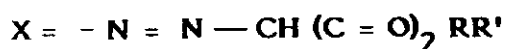
In the fourth series of compounds (IV), the $\nu_{\text{C=O}}$ band is located at 1640 and 1672 cm^{-1} for IV_a and IV_b whereas the $\nu_{\text{C=C}}$ bands are found at 1598 and 1620 cm^{-1} respectively. In the same order the C=N bond deformation leads to the band appearing at 1505, 1509 cm^{-1} for IV_a and IV_b respectively. The position of the bands due to $\nu_{\text{C=O}}$ as well as that of ν_{OH} at lower frequency may give a qualitative indication to the strength of the intramolecular hydrogen bond occurring. The appearance of the $\nu_{\text{C=N}}$ band for all compounds gives an indication that $\text{azo} \rightleftharpoons \text{hydrazo}$ as well as $\text{azo- hydrazone equilibrium}$ is liable to take place which can be represented as follows :



azo-hydrazone equilibrium



azo-hydrazo equilibrium



Spectra in the range 1500-1000 cm^{-1} :

This region is of interest, since the bands observed are symmetric stretching vibration of N=N group, in - plane bending or deformation modes of O-H group, in-plane deformation of aromatic C-H and the stretching modes of the C-O. The data are recorded in Table (19). The ir-spectra of the components of I, II, III and IV reveal medium or weak intensity bands around 1425-1389 cm^{-1} due to the symmetric vibration of the N=N group. The bands having three or four peaks around 1380-1300 cm^{-1} are corresponding to the in-plane bending modes of the O-H. Also, a band around 1158-1028 cm^{-1} is observed corresponding to the stretching vibration of C-O and that around 1253-1180 cm^{-1} for the in-plane deformation mode of aromatic C-H bonds.

Spectra in the range 1000-250 cm^{-1} :

Most of the strong bands appearing in the 1000-250 cm^{-1} region in the spectra of the dyes under investigation are attributed to the out of plane deformation vibrations of the aromatic C-H bonds. The position of the bands, in relation to the various types of substitution at the phenyl-azo or phenyl-bis-azo, can be discussed in terms of the number of adjacent hydrogen atoms attached to the rings. The ir-spectra of all compounds show a strong band in the region 995-600 cm^{-1} corresponding to the out of plane deformation of the aromatic hydrogen atoms .

Table (19) : Assignment of the vibration spectra of some functional groups of mono- and bis-azo-compounds.

assignment	I _a	I _b	I _c	II _a	II _b	II _c	III _a	III _b	III _c	IV _a	IV _b
ν_{OH}	3000 (b)	3360 (s)	3080 (b)	—	—	—	3400 (wb)	3360 (b)	3060	3480 (b)	3440 (b)
$\nu_{OH}^{of CO_2H}$	—	—	—	3020 (b)	3400 (b)	3130 (b)	—	—	—	—	—
$\nu_{C-H}^{of CH_3}$	2875 (m)	3000 (w)	—	2995 (b)	3030 (m)	—	2820 (w)	2930 (w)	—	2930 (w)	2925 (w)
$\nu_{C=O}$ assym.	1631 (vs)	1646 (vs)	1621 (s)	1700 (vs)	1641 (s)	1679 (vs)	1648 (s)	1675 (s)	1644 (m)	1640 (s)	1672 (s)
$\nu_{C=C}$ conjugation assym.	1599 (s)	1620 (m)	1597 (s)	1635 (vs)	1622 (w)	1639 (vs)	1600 (s)	1603 (s)	1598 (vs)	1598 (s)	1620 (m)
$\delta_{C=N}$ assym.	1509 (vs)	1512 (s)	1517 (sb)	1578 (s)	1582 (s)	1574 (s)	1510 (vs)	1509 (vs)	1510 (vs)	1505 (vs)	1509 (vs)
str. N=N sym.	1419 (w)	1410 (w)	1393 (w)	1412 (w)	1389 (m)	1404 (m)	1418 (w)	1412 (w)	1400 sh	1415 (w)	1425 (b)
δ_{O-H}	1368 (vs)	1380 (s)	1342 (sb)	1324 (vs)	1332 (s)	1335 (vs)	1365 (m)	1358 (s)	1328 (s)	1368 (m)	1360 (s)
β_{C-H} aromatic sym.	1238 (s)	1205 (vs)	1234 (s)	1220 (m)	1253 (m)	1228 (s)	1192 (m)	1180 (s)	1210 (s)	1200 (b)	1180 (s)
ν_{C-O} sym.	1158 (s)	1138 (s)	1152 (m)	1138 (s)	1130 (s)	1080 (s)	1127	1125 (vw)	1153 (m)	1028 (m)	1052 (m)
γ_{C-H} aromatic sym. and assym.	938 (885- 730)	983 (887- 700)	995 (900- 700)	984 (938- 700)	982 (892- 600)	988 (938- 600)	980 (878- 690)	980 (931- 600)	990 (930- 684)	980 (885- 600)	982 (932- 615)

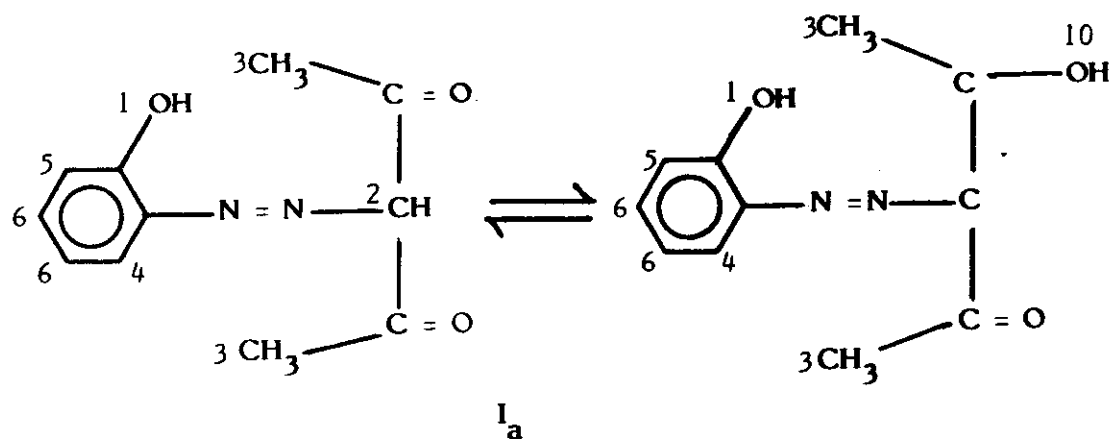
s = strong, b = broadened, m = medium, w = weak, sh = shoulder, β = in plane deformation, γ = out of plane deformation, ν = stretching, δ = deformation.

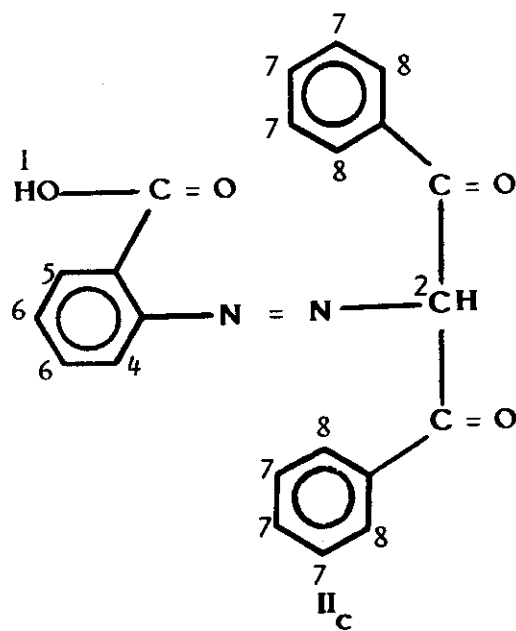
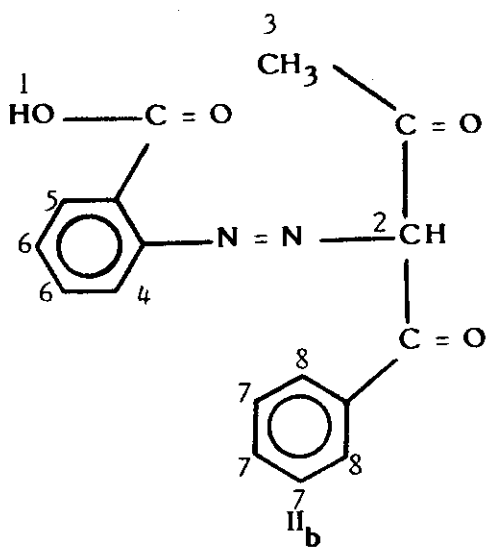
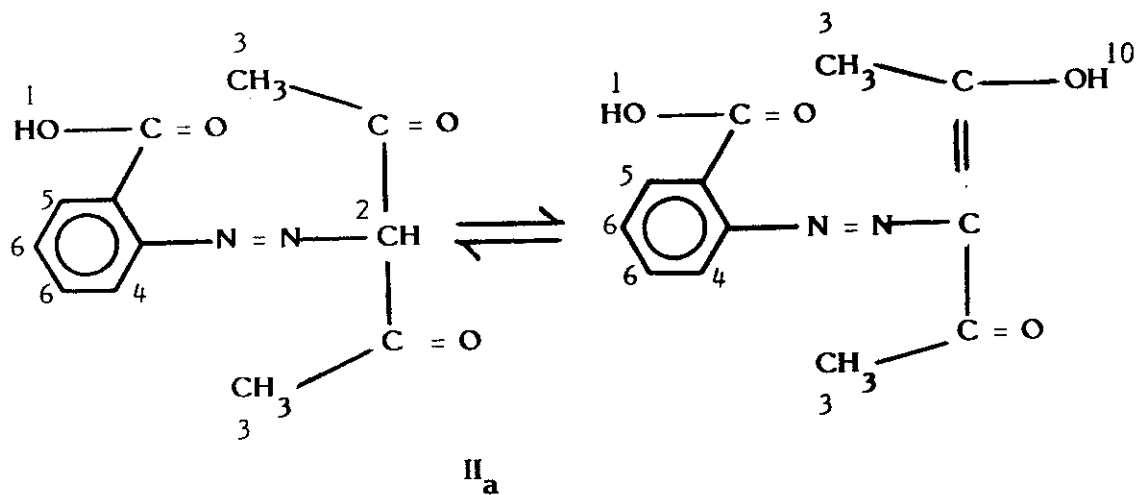
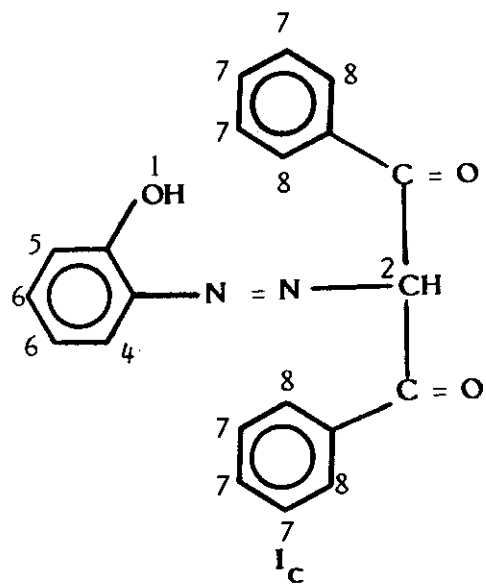
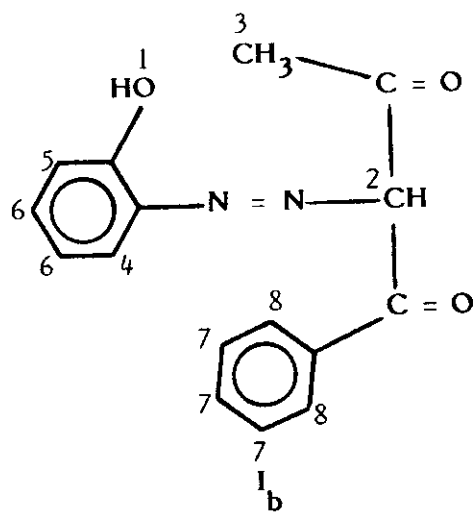
^1H NMR - spectra of some azo dyes

A further support for the conclusion obtained from the C, H, N elemental analysis and IR or UV-visible spectra for the structure of these azo compounds is gained by a consideration of their ^1H nmr- spectra. The signals due to the protons of the OH groups (enolic form or that attached to the phenyl ring) and the effect of substituents (from methyl group to phenyl ring in the diketone part of the molecule) on the position of it are studied. The ^1H nmr spectra of acetylacetonethioxythiocarbonylhydrazone was studied⁽⁸⁸⁾. Issa et. al.⁽⁸⁹⁾ investigated also the ^1H nmr- spectra of some azo-hydrazone dyes. The position of the signals observed in the spectra due to the different types of the protons of the molecules were discussed.

^1H nmr spectra of o-hydroxy and o-carboxyphenylazo- β -diketones (I_{a-c}), (II_{a-c}):

The different types of hydrogen protons which are expected for the compounds under investigation can be formulated as follows :





The ^1H nmr spectra of the compounds $\text{I}_{\text{a-c}}$ are shown in Figs. (53-55) and the chemical shift of the different types of protons are recorded in Table (20). The proton magnetic resonance spectra of I_{a} , I_{b} after deuteration with D_2O are also shown in Figs. (53,54), the fine structure of the spectrum has been taken but the coupling constant for the spin-spin coupling are not evaluated. All signals observed take the integration value for its area which give evidence and helps to assign the signals. It is clear from the spectral curves of I_{a} and I_{b} that the signals lying at very downfield side 14.66 and 14.6 ppm or at 10.47 and 12.6 ppm respectively are removed after deuteration which give evidence that they are due to the proton of OH groups attached to the phenyl ring and to -OH group of the enol form of the compound respectively. This supports the previous indication from IR spectra that the keto-enol form equilibrium is liable to exist under this condition. The signal of the o-OH groups is shifted to higher field when the CH_3 group is substituted by phenyl ring.

The proton 4 has single ortho and meta coupling as that of proton 5 whereas proton 6 has double ortho and meta coupling. The signal of proton 4 is at magnetic field more than that of 5 and both are more than that of proton 6 which is shown at downfield.

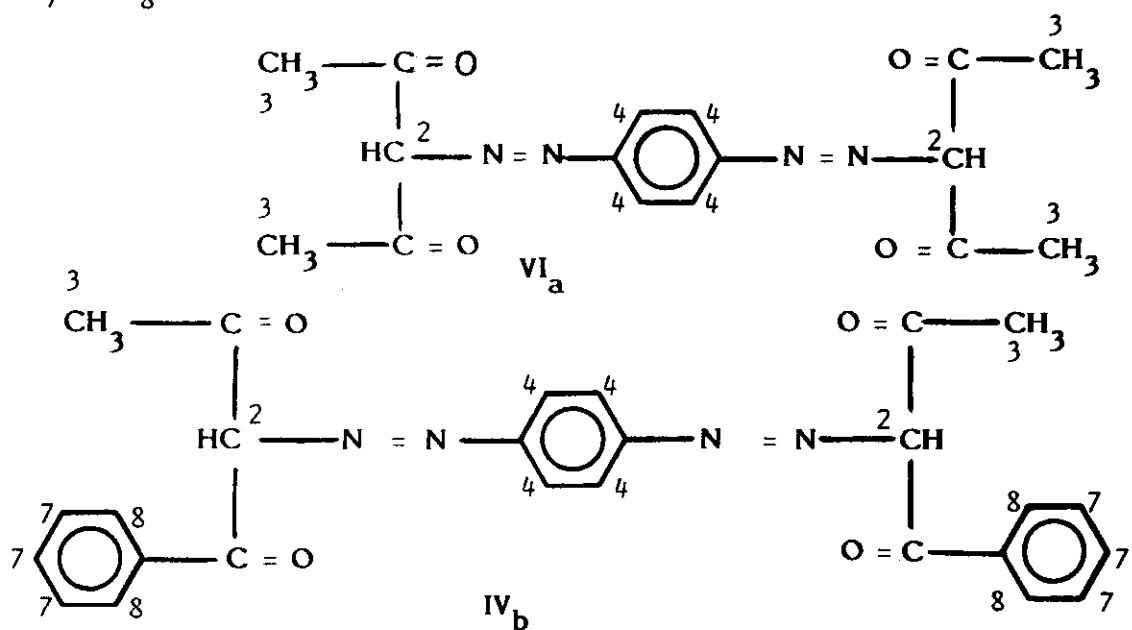
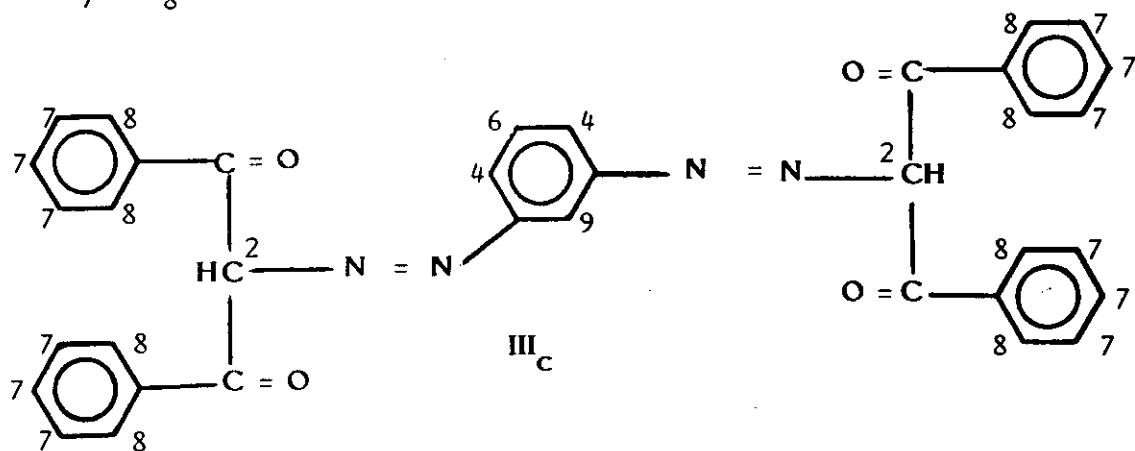
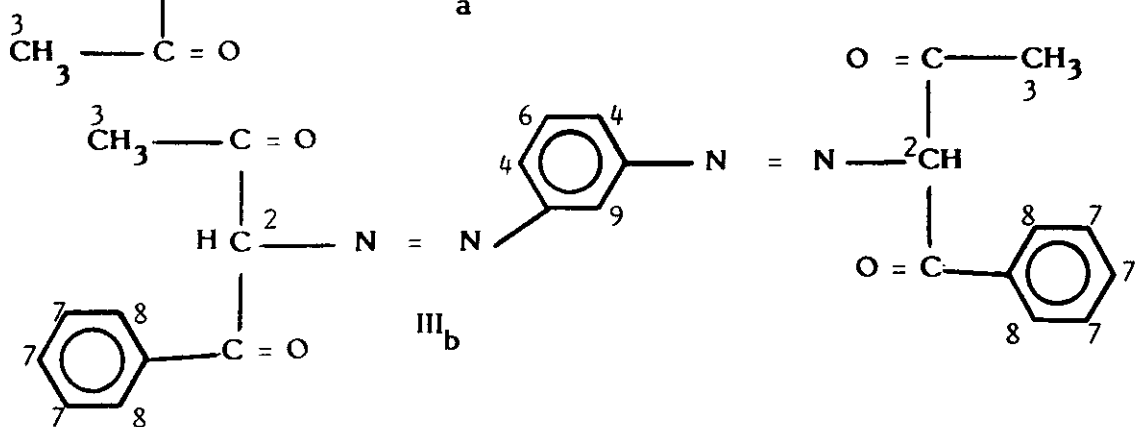
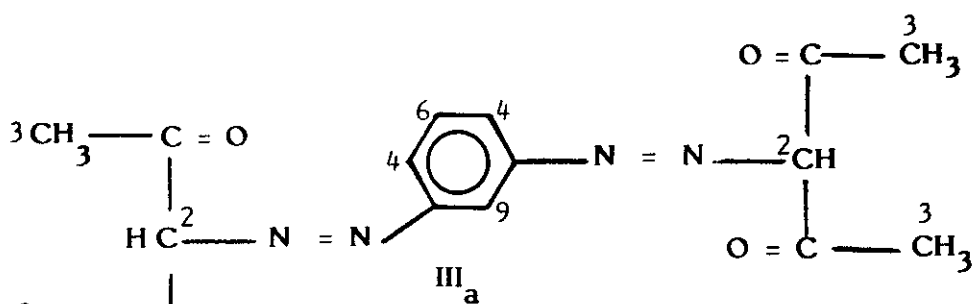
The signal due to the methine proton of the acetylacetone part of the molecule appears at chemical shift 2.2-3.33 ppm. On going from ligand I_{a} to I_{b} or I_{c} a new signal at downfield appeared which is due to the protons of the phenyl group. These signals become very intense and more shifted downfield in case of I_{c} than of I_{b} .

The ^1H nmr spectra of II_{a-c} as well as its deuteration, II_a by D_2O , are shown in Fig. (56) and chemical shifts of the different signals are recorded in Table (20). The proton 1 of carboxylic group (Figs. 56-58), exhibits a signal at 8.0, 7.9 and 4.26 ppm for II_a , II_b and II_c respectively. This was substantiated by the removal of the signal on deuteration. Such position is due to the low shielding of the carboxyl group which shift the signal towards up-fields.

The ^1H nmr signal at very downfield (13.0-13.75 ppm) which is also removed by deuteration is due to the proton of the -OH group established from the keto \leftrightarrow enol tautomerism. The signal of the methyl group of II_b is at higher field than that of II_a which may be due to the substitution of the second CH_3 group by the ph one. The proton of the phenyl ring ortho to azo which has ortho and meta coupling exhibits a signal at downfield than that of the corresponding proton ortho to the carboxylic one. Proton 8 attached ortho to the carbonyl group is at downfield than that of proton 7 due to the electron acceptor effect of the $\text{C}=\text{O}$ group. it can be noticed that the nmr studies have shown that the phenolic or the carboxylic hydrogen atom, which give peaks at far downfield, must be strongly hydrogen bonded⁽⁹⁰⁾.

^1H nmr - spectra of m- and p-bis-azobenzene-di- β -diketones (III_{a-c} and $\text{IV}_{a,b}$) :

The bis-azo dyes have different hydrogen types which can be formulated as follows :



The ^1H nmr spectra of III_{a-c} and $\text{IV}_{a,b}$ are shown in Figs. (81-85) and the magnitude of the chemical shifts of the different types of protons are recorded in Table (20). The ^1H nmr spectra exhibit a weak signal at chemical shift 13.55, 14.68 and 14.74 ppm for compounds III_a , III_b and III_c respectively. This signal is removed by deuteration. At the same time another signal appears at 1.9-2.2 ppm range. This indicates that the first one is due to the -OH group whereas the second to the methine group (-CH) and confirming the presence of the keto-enol equilibrium in the medium. Proton 9 has only meta coupling and its signal is shown at very high fields in the spectrum supporting the presence of this proton ortho to the azo group. Proton 4 has ortho and meta coupling whereas that of 6 is only ortho coupling. As that of mono-azo dyes the proton 8 exhibits its signal at lower field than that of proton 7 due to the electron acceptor properties of the C=O group.

It is clear from the spectra that the signal of the protons of CH_3 of compound III_a is of high integration area which decreased in III_b and disappeared in case of III_c . This behaviour is shown also in case of the compounds $\text{IV}_{a,b}$, but in this case the proton 4 (Figs. 84,85) is only ortho coupling and gives a very intense signal at high fields. The signal of the proton of the methyl group is affected by the substitution of the second CH_3 group by ph one which leads to shift it to the higher field side of the spectrum. It is generally concluded that the keto - enol equilibrium of these compounds is established as well as the presence of the intramolecular hydrogen bond between the OH or COOH protons and the -N=N- group.

Table (20) : Assignment and chemical shifts (ppm) of the different types of protons of the mono- and bis-azo-dyes.

compound	chemical shift (δ) ppm of protons									
	H ¹	H ²	H ³	H ⁴	H ⁵	H ⁶	H ⁷	H ⁸	H ⁹	H ¹⁰ (-C-OH)
I _a	14.66	3.35	2.4	7.63	7.73	7.0	—	—	—	10.47
I _b	14.6	2.2	2.48	7.07	7.18	6.95	7.8	7.53	—	12.6
I _c	3.35	2.45	—	6.81	6.97	6.7	8.1	7.5	—	—
II _a	8.0	3.25	2.35	7.9	7.15	7.56	—	—	—	13.0
II _b	7.9	3.2	2.3	7.1	7.25	6.8	7.8	7.4	—	13.18
II _c	4.26	1.9	—	7.13	7.23	7.07	8.12	7.57	—	13.75
III _a	—	1.9	2.53	7.4	—	7.75	—	—	6.74	14.68
III _b	—	2.2	2.68	7.15	—	6.25	7.99	7.6	7.34	14.74
III _c	—	—	—	7.44	—	6.9	8.2	7.7	7.51	13.55
IV _a	—	—	2.5	7.52	—	—	—	—	—	14.98
IV _b	—	3.52	2.2	6.43	—	—	7.95	7.62	—	8.2